RSC Advances

REVIEW

View Article Online
View Journal | View Issue

Cite this: *RSC Adv.*, 2024, **14**, 7806

Overall perspective of electrospun semiconductor metal oxides as high-performance gas sensor materials for NO_x detection

Niloufar Khomarloo,*[abc] Elham Mohsenzadeh,[bc] Hayriye Gidik,[bc] Roohollah Bagherzadeh *[a] and Masoud Latifi[d]

Received 27th November 2023
Accepted 18th February 2024

DOI: 10.1039/d3ra08119b

rsc.li/rsc-advances

Gas sensors based on nanostructured semiconductor metal oxide (SMO) materials have been extensively investigated as key components due to their advantages over other materials, namely, high sensitivity, stability, affordability, rapid response and simplicity. However, the difficulty of working at high temperatures, response in lower concentration and their selectivity are huge challenges of SMO materials for detecting gases. Therefore, researchers have not stopped their quest to develop new gas sensors based on SMOs with higher performance. This paper begins by highlighting the importance of nitrogen monoxide (NO) and nitrogen dioxide (NO_2) detection for human health and addresses the challenges associated with existing methods in effectively detecting them. Subsequently, the mechanism of SMO gas sensors, analysis of their structure and fabrication techniques focusing on electrospinning technique, as well as their advantages, difficulties, and structural design challenges are discussed. Research on enhancing the sensing performance through tuning the fabrication parameters are summarized as well. Finally, the problems and potential of SMO based gas sensors to detect NO_x are revealed, and the future possibilities are stated.

1 Introduction

Gas sensing technologies play a critical role in various applications, particularly in the field of healthcare. In which NO and NO_2 are two specific target gases with great significance in this field. Among gas sensors, SMO based gas sensors have received remarkable attention owing to their unique properties, such as high sensitivity, simple fabrication, miniaturization, portability, and real-time monitoring. They are widely used as commercial sensors as they exhibit a wide range of electronic, chemical, and physical properties.[1,2] SMO gas sensors operate based on the adsorption and desorption processes occurring on the surface of the sensing material when interacting with the target gas molecules. The movement of electrons and holes is affected by the size and geometry of the materials; therefore, the sensing layer usually determines the sensitivity and selectivity.

Based on this, nanostructured SMOs have garnered significant attention[3] as they have new physical and chemical properties and large specific surface areas with numerous active sites, which facilitate fast adsorption and reaction of target gases.[4–6] Nanofibers as one of the nanostructures, enhance sensing performance including high sensitivity, and rapid response. A nanofiber mat, forming a gas-sensitive layer is characterized by high porosity and a large surface-to-volume ratio, in addition, the metal oxide crystallites in nanofibers can be extremely small in size.[7] Among different strategies to form nanofibers,[8–10] their fabrication through the electrospinning technique have emerged as a promising platform for enhancing the performance of gas sensors.[11] These nanofibers possess unique morphological and structural characteristics that significantly influence the sensitivity, selectivity, and stability of the sensors. Electrospinning offers numerous benefits for gas sensor development, including high crystalline structure, the potential for noble metal doping, competitive production rates, and the ability to create diverse structures such as core–shell and hollow.[12] In this review, we focus on the electrospinning process for SMOs nanofiber production to detect nitrogen monoxide (NO) and nitrogen dioxide (NO_2). In controlling the size and uniformity of the nanofibers, polymers are employed during the preparation of the precursor. Subsequently, the electrospun membrane is subjected to a calcination process to obtain the final nanofibrous SMO materials.[7] There is extensive research on developing sensitive and selective gas sensors for different applications using nanofibers through the

[a]*Advanced Fibrous Materials Lab (AFM-LAB), Institute for Advanced Textile Materials and Technology, Amirkabir University of Technology (Tehran Polytechnic), Iran. E-mail: khomarloo1@gmail.com; bagherzadeh_r@aut.ac.ir*

[b]*Univ. Lille, ENSAIT, Laboratoire Génie et Matériaux Textile (GEMTEX), F-59000 Lille, France*

[c]*Junia, F-59000 Lille, France*

[d]*Textile Engineering Department, Textile Research and Excellence Centers, Amirkabir University of Technology (Tehran Polytechnic), Tehran, Iran*

electrospinning method.[13] Nonetheless, only few of the studies focus on detecting NO.

In this review, we consider NO_2 gas since NO is highly reactive leading to its conversion into NO_2.[14,15] Moreover, prolonged exposure to NO_2 levels exceeding 3 ppm for more than 8 hours can result in severe respiratory complications.[16] Therefore, it is crucial to take measures to prevent such exposure. Furthermore, we delve into the influence of electrospinning parameters on the formation of nanofiber structures, considering that detection in resistive-type gas sensors, relies on the surface adsorption and desorption processes. Therefore, surface morphology, sensing layer structures and its composition is of great importance in interactions with target gas molecules. We provide a comprehensive overview of common metal oxide nanofibers and their composites with other materials, all fabricated using the electrospinning method, focusing specifically on NO and NO_2 detection. Finally, future perspectives and potential strategies to enhance nanofiber structures through optimization techniques are proposed and improved preparation methods are addressed. Future advancements aim to significantly improve the performance of metal oxide gas sensors in detecting NO_x gas. Henceforth, the implications of this research are far-reaching and hold great promise for advancing healthcare technologies.

2 Importance of detecting NO and NO_2 gases

Asthma, also called bronchial asthma, is a heterogeneous disease diagnosed by the presence of intermittent symptoms of wheezing, coughing, and chest tightness, typically related to reversible airflow obstruction, usually resolves spontaneously or with asthma treatment.[17] Over the years, clinicians have defined several phenotypes based on the presentation and age of onset of symptoms, the severity of the disease, and the presence of other conditions such as allergy and eosinophilia with different long-term outcomes and responses to therapy with corticosteroids.[18] Despite the recognition of these phenotypes of asthma, the approach to the management of asthma recommended by the International Global Initiative for Asthma (GINA) guidelines continues to be, based on the severity of the condition, with drugs based on asthma control.[19] Asthma affects more than 235 million people in the world. This total includes more than 5 million children just in the US. Asthma can be life-threatening if not treated, also, this respiratory disease is a chronic, ongoing, condition, meaning it doesn't go away and needs ongoing medical management. In addition to financial costs, asthma has a long-term impact on the quality of life of susceptible individuals.[20]

NO_2 is an oxidizing gas, which is considered to be the most dangerous and toxic gas that should be controlled. In the process of industrial development, waste gases will inevitably be produced, including nitrogen compounds. Among these waste gases, NO_2 can cause the human body to infect some respiratory diseases, such as asthma. The Health and Safety Rule Alarm mentioned that the human body cannot stay more than 8 h in an environment with 3 ppm NO_2.[21–23] Thus, NO_2 is considered to be one of the most dangerous gases and the environmental pollution of this gas has become a global issue. Therefore, it plays a key role in monitoring industrial waste gas that develops excellent NO_2 gas sensors.[24]

NO as an oxidizing gas, plays a key role in lung biology and an inflammatory mediator is produced in the lung from nitric oxide synthases during the conversion of the amino acid L-arginine to L-citrulline. NO is a biomarker of respiratory disease such as asthma and it is normally produced by the human respiratory system.[25] A biomarker is a measurable indicator that can evaluate normal or pathological biological processes or pharmacologic responses to a therapeutic intervention.[18] The fractional exhaled nitric oxide (FeNO) biomarker originated from nitric oxide production by the airway epithelium as a result of inducible nitric oxide synthase upregulation during the process of allergic inflammation.[26] Diagnostic methods to detect respiratory disease are not only costly but are also invasive, thereby adding to people's stress. To diagnose the disease before it becomes chronic, measuring the FeNO is one solution which can be performed easily and close to real-time.[27] In conjunction with symptom scores and lung function tests, FeNO measurement could provide a more useful and effective approach for the identification of asthma and other corticosteroid-responsive inflammatory airway conditions.[28,29] Unfortunately, technologies like chromatography-mass spectroscopy require site and bulky equipment, highly trained personnel, and time-consuming preconcentration of samples, all of which impede its use as a screening tool.[30]

Therefore, measuring the concentration of NO in exhaled breath by nanostructured SMO gas sensors (Fig. 1) can help overcome costly, invasive, and complicated methods which are used nowadays.[20,25,31–37] To further explain the process of SMO based gas sensors, the next section comprehensively elaborates on their properties and structure.

3 Sensing mechanisms, heterojunction strategies, and considerations for enhanced NO and NO_2 detection

Gas sensors can be classified into electrochemical, optical, thermoelectrical, electrical, and piezoelectric. Among these

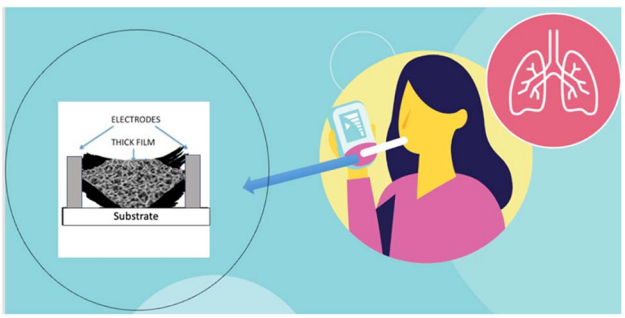

Fig. 1 Schematic of non-invasive and easy-to-use sensor based on SMOs nanofibers to detect gases in exhale.

types, the mechanism of SMOs is based on chemiresistive gas sensors. These gas sensors are electrical and can be produced by metal oxide, conductive polymers[22,23] carbon nanotubes, and their composites.[38] Compared to carbon materials and organic materials, SMOs generally have higher sensitivity, faster response/recovery speed, better reversibility and stability, and they are cost-effective with simple fabrication processes.[5] While polymer-based chemiresistors offer several advantages *e.g.*, low power consumption, small size, low operating temperature, and low cost, their sensitivity depends on the type of coating and they also show a drift in baseline due to polymer instability.[39]

Therefore, here we focused on SMO as a promising material for highly sensitive gas sensors.[40] Pristine metal oxides exhibit not only high working temperatures but also limited response[41,42] and poor selectivity[43–45] as highlighted in various published articles. To enhance the detection of harmful gases, achieving high response and selectivity becomes particularly crucial. In pursuit of improved gas sensing performance for metal oxides, researchers have explored numerous approaches, including morphology regulation,[46–48] preparation methods, doping activation by external light sources, and composite materials.[24,49,50] Various nanostructures and types of SMO sensing materials have been successfully employed to address these limitations. Among them, one-dimensional (1D) nanostructured sensing materials such as nanofibers, nanowires, and nanorods have gained significant preference for gas sensor development. This preference stems from their inherently higher surface-area-to-volume ratio, which allows for enhanced absorption of the target gas. Additionally, the broader interaction zone across the cross-sectional area enables a more pronounced modulation of electrical properties upon exposure to analytes.[51]

At the same time, different strategies such as the doping effect, formation of heterojunction, *etc.*, have been researched for tuning the chemical nature, materials structure, and electronic properties of 1D nanostructure sensing materials which further optimized sensitivity, selectivity, operating temperature, and so on.[24,51] SMOs are categorized into n-type and p-type. Beyond n-type or p-type metal oxide as a sensing material, combining metal oxides with other metal oxides, noble metals, and carbon-based materials might generate p–p, n–p, and n–n-type heterojunctions and potentially further enhance electron mobility.[1] Fabrication of n–n junctions with the addition of n-type semiconductors such as zinc oxide (ZnO),[52] tin(IV)oxide (SnO_2), molybdenum trioxide (MoO_3), and ceric oxide (CeO_2), and p–n junctions with the addition of p-type semiconductors such as NiO, Co_3O_4 and PdO showed high responses.[52] ZnO, titanium dioxide (TiO_2), tungsten trioxide (WO_3), and SnO_2 are the most common SMOs. The subsequent section elucidates the specifications required for a dependable gas sensor and outlines the sensing mechanism employed for NO and NO_2, which are oxidizing gases, using p-type and n-type SMOs. Subsequently, the structural characteristics and sensitivity of electrospun SMO nanofibers towards NO and NO_2 are compiled and analyzed.

Nanomaterials-based gas must be capable of detecting trace concentrations of gases sensitively and selectively, even in the presence of interfering environmental or physiological factors.[17] There are several requirements which are summarized as follows.

1. Strong anti-interference ability. Gas sensors must be immune to the high humidity and other interfering gases in exhaled breath, ensuring the accuracy and reliability of breath analyses.

2. High sensitivity and low limit of detection (LOD). Gas sensors must be able to recognize low-concentration biomarkers of the disease, even at single-molecule level.

3. Strong stability. Exposed to the same respiratory gas sample, gas sensors must exhibit consistent results.

4. Rapid and real-time gas sensors must respond to biomarkers quickly, saving time compared to bulky equipment (*i.e.*, GC-MS).

5. Good interaction. Gas sensing systems should have a friendly human/computer interface. The test results should be clear and visual, the experimental parameters should be tunable, and the operation should be simple. As noninvasive detection techniques, gas sensors play an important role in breath diagnosis. Therefore, great efforts have been made to design and develop novel gas sensors.

In this regard, to enhance the performance of NO gas sensors, studies should work on increasing their sensitivity, selectivity, and lower working temperature to detect low gas concentrations. To measure the capability of sensors, the sensing layer is exposed directly to the gas. The interaction between the target gas and sensing layer modulates the electrical resistance of the gas sensor, resulting in the generation of a sensing signal. This conductivity change is due to variations in the width of the electron depletion layer across the exposed area of the sensing layer.[53] The response of the n-types gas sensors to oxidizing gases such as NO and NO_2 is defined by the ratio of R_g/R_a and for p-type SMOs is R_a/R_g. Here, R_a is the original base resistance of the sensor in air, and R_g is the stabilized resistance of the sensor in the presence of the applied gas.[54]

Selectivity is the ability of the gas sensors to detect a specific gas in a mixture of gases. The response time (τ_{res}) is defined as the time in which the resistance of the sensor changes to 90% of the original base resistance, and the recovery time (τ_{rec}) is defined as the time needed until 90% of the signal is recovered.[55,56] Repeatability is one of the significant features of gas sensors in practical applications. If a sensor shows large variations in response over sequential cycles, it may fail to detect a specific gas accurately. Based on the Liu model, the sensor properties are formulated as functions of grain size, depletion layer width, film thickness, oxygen vacancy density, gas concentration, pore size as well as operating temperature.[57] The prevailing theory regarding the mechanism of gas sensing involves the adsorption of oxygen and is widely accepted in scientific circles.[12] According to this theory, when a sensor is exposed to air, oxygen molecules interact with semiconductors, causing the capture of electrons and the subsequent formation of oxygen anions. The nature of these oxygen anions is influenced by the operating temperature. At temperatures below 147 °C, the predominant form of oxygen anions is O_2^-. As the temperature rises, the O_2^- species transforms, leading to the

formation of O^-. At temperatures exceeding 397 °C, the oxygen anions are further converted into O^{2-}.[48–50,58]

In the n-type metal oxide gas sensors adsorbed air oxygen onto the metal oxide receives electrons from metal oxide *via* conduction bands. This electron transformation causes a reduction in carrier charges in the metal-oxide surface and the formation of the depletion layer and the formation of oxygen ions. The reducing target gas takes electrons from oxygen and transports electrons to the conduction band of metal oxides resulting in an increasing conductivity and reducing resistance. In the case of exposure to the oxidizing target gas like NO and NO_2, the overall result reduces the conductivity and increases the depletion layer (Fig. 2).[50–53,59] In the p-type metal oxide, the adsorbed oxygen traps the electron through the valence band of metal oxide which results in generation holes. The effect of exposure to the reducing or oxidizing target gases on the conductivity is the reverse of n-type cases.[1,12]

The surface band bending on SMOs nanofibers occurs due to the chemisorption of oxygen species in the air. As the concentrations of NO and NO_2 increase, there is a gradual accumulation of adsorbates on the material's surface, leading to a slower return of resistance to its initial state at lower concentrations. This slight deviation in resistance values is attributed to kinetic inhibition processes at room temperature.

Addressing the challenge of NO gas converting to NO_2 in the sensing mechanism, research employs strategies to ensure comprehensive detection of all NO molecules.[14,15] The NO_2 sensing mechanism is considered, involving reactions between NO molecules and available oxygen species, resulting in the formation of nitrite and/or nitrate species. This increases the overall resistance of the sensor. The adsorption and desorption rates of NO are influenced by activation energy, dependent on the operating temperature. Temperature-dependent processes, such as the formation of N–N bonds and intermediate $N_2O_2^{2-}$(ads) species, contribute to the generation of N_2O and O^-(ads), reacting with NO to form NO_2. The release of electrons is observed during these processes, influenced by the sensor's operating temperature.[60]

The interaction of n-type semiconductor oxides with NO_2 in dry air, leading to a decrease in electrical conductivity, can be described by specific reactions:[61]

$$NO_2\ (gas) \leftrightarrow NO_2\ (ads) \quad (1)$$

$$NO_2\ (gas) + e^- \leftrightarrow NO_2^-(ads) \quad (2)$$

$$2NO_2\ (gas) + 1/2\ O_2\ (gas) + 2e^- \leftrightarrow NO_2^-\ (ads) + NO_3^-\ (ads) \quad (3)$$

$$NO_2^-\ (ads) + 1/2\ O_2\ (gas) \leftrightarrow NO_3^-\ (ads) \quad (4)$$

In Nasriddinov *et al.*'s[61] studies, the sensitivity of hybrid materials towards NO was found lower than NO_2. The interaction between SMO surfaces and NO/NO_2 follows a similar mechanism, involving adsorption and the localization of electrons from the semiconductor conduction band. The lower sensitivity of hybrid materials towards NO, compared to NO_2, can be attributed to distinct initial steps in the detection process. The reaction with NO_2 involves a straightforward one-electron reduction (reaction (7)), benefiting from the strong oxidative properties of nitrogen dioxide. On the other hand, the interaction with NO (reaction (5)) primarily involves the oxidation of the target gas facilitated by oxygen on the semiconductor oxide surface.

This fundamental difference in mechanisms likely explains the disparate sensitivities to NO_2 and NO, despite the generation of similar surface species in both pathways. Additionally, an increase in relative humidity (RH) within the range of 0–90% leads to a decline in baseline resistance for all materials, as well as modifications in the sensor signal during the interaction with nitrogen oxides. Furthermore, the heterojunction exhibits modulation at the junction, which manifests as alterations in both the depletion region and potential barrier. In contrast to junctions comprised solely of n-type materials, the trapping and release of electrons from the conduction band play a more significant role in modifying the potential barrier and depletion region established by the junction.[8] The heterojunction demands an equilibrium while this equilibrium is disrupted when the density of electrons is and just, the system must adjust and return to a steady state, giving us more sensitive responses.[62] Reducing gases will grow the depletion region and cause more bend banding, growing the potential barrier, as more electron density decreases in the conduction band. Oxidizing gases would have the opposite effect.[48–50]

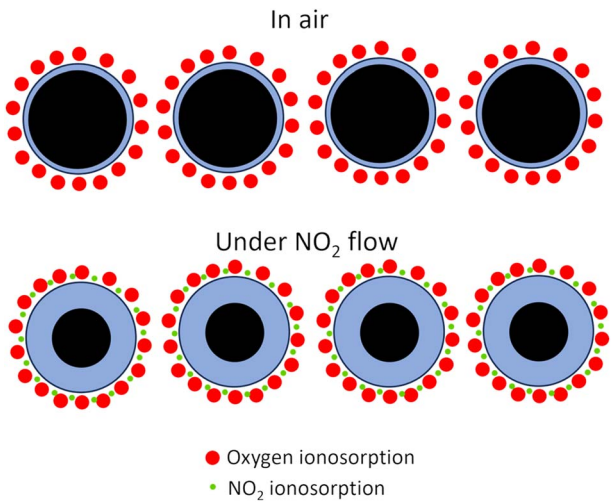

Fig. 2 Schematic representation of the outer depletion region and inner conduction region.

4 Optimizing sensitivity through electrospun nanofibers: a comprehensive exploration of morphological factors and applications in NO and NO_2 gas detection

1D nanostructured sensing materials, such as nanofibers, offer immense potential for enhancing sensitivity in gas sensors.

This is primarily attributed to their large surface-area-to-volume ratio, which enables the presence of numerous reactive sites. The abundant reactive sites facilitate effective charge carrier transport and promote high surface energy, contributing to improved sensitivity in gas sensing applications.[63,64] Gas sensing performance is influenced by the structure and the morphology of nanofibers such as diameter, grain size, and crystallinity. Smaller diameters offer a larger surface-to-volume ratio, resulting in increased active sites, efficient charge carrier transport, and higher surface energy.[63]

In nanofibers, smaller crystallite sizes that approach the Debye radius have a significant impact on gas sensing. They result in a maximized resistance change of the sensing material upon exposure to air, leading to a substantial variation in the electrical signal. Consequently, when exposed to the analyte, the electrical signal variation reaches its maximum value. This behavior highlights the importance of achieving smaller crystallite sizes in nanofibers for optimizing gas sensing performance.[65]

Furthermore, it is essential to strike a balance between grain size and sensitivity in gas sensing. Increasing the grain size can lead to a decrease in sensitivity. However, it also results in improved crystallinity, which contributes to the overall gas sensing performance. Achieving the optimal balance between grain size and sensitivity is crucial to enhance the gas-sensing capabilities of the material. There are several materials synthetic methods to produce a broad variety of nanofibers sensing materials based on SMOs, such as melt-blown,[66,67] self-assembly,[68] solution blow spinning,[67] force spinning,[69] and electrospinning.[70] Electrospinning is a straightforward,[55] versatile, and low-cost route to produce different kinds of nanocrystalline metal oxides with a highly porous fibrous morphology.[11,71,72] Therefore, this technique is favored in producing nanofibers due to its flexibility in having different structures and applying numerous materials. For this reason, chemiresistive sensors depend on materials and structure and this technique has the potential to detect gasses such as NO and NO_2 which are challenging in low concentrations.[55]

Moreover, with the increasing number of electrospinning companies in recent years, it is expected to move progressively from a laboratory bench process to an industrial-saleable process. From a commercial point of view, electrospinning is the only method of choice for the large-scale preparation of nanofibers compared to other available methods, due to the easy handling, minimum consumption of solution, controllable nanofiber diameter, low cost, simple, and reproducible nature in processing nanofibers as well as technical advances over other methods (scale up the process). Accordingly, composite metal oxides can be produced easily and massively on a commercial scale by a straightforward, very low-cost, versatile, and facile electrospinning process.[55]

Among different morphologies, porous nanostructures composed of nanograins with small final diameters ($D \leq$ Debye length) have a profound impact on enhancing effective gas adsorption and diffusion. This, in turn, significantly increases the sensitivity of the sensor.[55,73–76] In addition to remarkably specific surface areas in electrospun nanofibers (one to two orders of magnitude larger than flat films), they possess high porosity (approximately 70–90%) owing to the presence of small and large pores. These characteristics render electrospun nanofibers highly attractive for designing ultra-sensitive sensors.[74,77] Additionally, the electrospinning technique enables the fabrication of ceramic nanofibers derived from various inorganic precursors/polymeric matrices, offering versatility in terms of different assemblies such as nanocomposites, core–shell structures, or hollow configurations.[78]

This review bridges the existing knowledge gap by focusing specifically on the sensitivity of electrospun nanofibers towards NO and NO_2 gases (Fig. 3). While there are previous reviews available on electrospinning SMOs and their sensitivity towards various gases, this review emphasizes the detection of NO gas and subsequently NO_2 using electrospun nanofibers. By examining the influence of electrospinning parameters on nanofiber structure, researchers can explore a new approach to developing SMO-gas sensors with controlled nanofiber structures that enhance surface-to-volume ratio for improved detection of NO and NO_2 gases. Furthermore, the review acknowledges the limited study on detecting NO at the ppb level, which holds significant relevance in disease diagnosis and monitoring.

4.1 Fine-tuning gas sensitivity: electrospinning parameters and structural optimization in metal oxide nanofibers

A typical setup for electrospinning consists of a high-voltage power supply (10–70 kV), spinneret with a metallic needle, solution reservoir, and grounded collection device,[7] as it is shown in Fig. 4.

The most important parameter is gas sensitivity, which still does not reveal the exact reasons, but it is strongly related to surface reactions.[54] SMOs nanofibers have large specific surface areas with numerous active sites, facilitating fast adsorption and the reaction of the target gases, thus enhancing their sensing performance.[5,24] Sensing layers containing nanorods and nanosheets require extensive processes such as high temperatures or special equipment for fabrication, while nanoparticles and nanofibers require relatively simple processes such as electrospinning.[80] As Metal oxides are not directly spinnable, they need to rely on the use of precursor solutions.[81] The size of the nanograins can be manipulated and changed according to the desired applications of the nanofibers by controlling the heat treatment conditions of heating temperature, heating time, heating and cooling rate. For gas sensing applications, the size of the nanograins must be optimized to obtain the best sensing performance.

Generally, nanofibers with smaller nanograins have better sensitivity and faster response than those with larger nanograins due to the higher surface area.[55] It's worth highlighting that nanofiber sensors offer a significant advantage in terms of reduced response and recovery times. This advantage is particularly important, as slow response and recovery times used to be a significant drawback of traditional gas sensors. This improvement can be attributed to the extensive surface area and heightened porosity of nanofiber-based sensitive materials. The remarkable porosity plays a crucial role in these

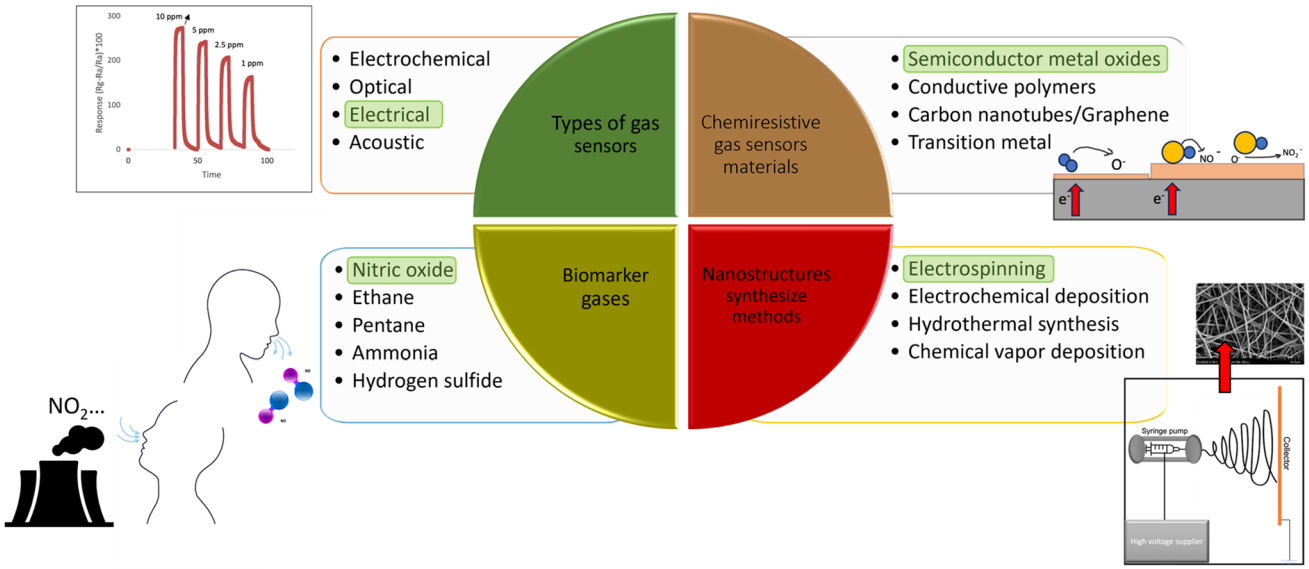

Fig. 3 Overview of research gap in detecting NO_x gas using electrospun nanofibers.

sensors, contributing to their exceptional operational characteristics, namely, rapid and excellent response rates when compared to conventional sensor materials. This distinctive structure enables the effective infiltration of the target gas into the porous structure of the ceramic layer, which is believed to be the primary reason behind the exceptional gas sensitivity exhibited by metal oxide gas sensors produced through this technique.[82] Unlike standard thin- and thick-film technologies that generate granular layers with densely packed nanoparticles, leading to inefficient gas transfer, electrospun sensors display a dual distribution of pore sizes, encompassing both small and large pores. This feature augments gas diffusion and increases the conductometric response of these layers.[98] The structure of as-spun nanofibers can be influenced by each step of the electrospinning process. In the subsequent section, we examine the key parameters of electrospinning that significantly impact the diameter and structure of SMO nanofibers.

4.2 The role of various variables in electrospun nanofibers

The optimization of electrospun fiber is based on the final application and the desire of researchers, which is about more surface-to-volume in sensing applications. To have control of the structure, it should be known that there are 6 forces needed to be considered for optimizing the parameters in the electrospinning method; (1) body or gravitational force, (2) electrostatic force (force exerting on charges carried within a jet segment when the jet is in an electrostatic field) which carries the charged jet from the needle to the collector, (3) coulombic stretching force (repulsion force between charges of mutual

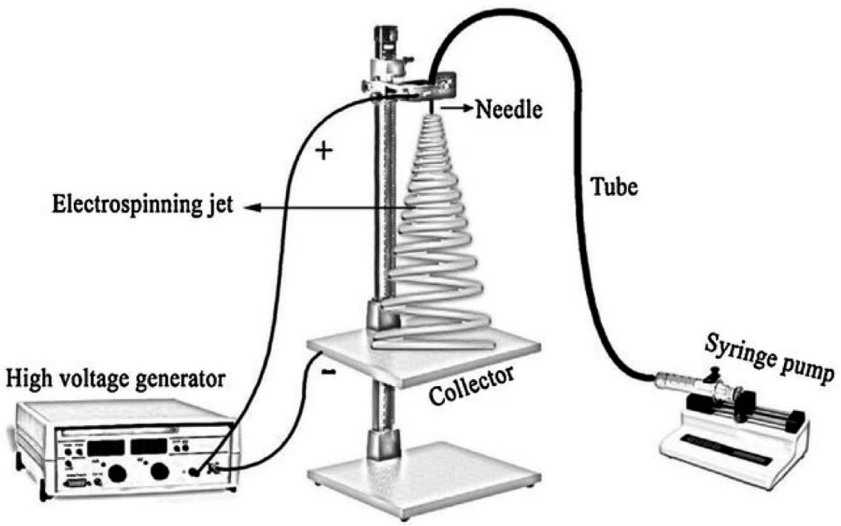

Fig. 4 Scheme of the home-made electrospinning setup.[79] Reproduced from (ref. 79) with permission from Elsevier, copyright 2016.

polarities) which tries to push apart adjacent charged species carried within the jet segment and is responsible for the thinning or the stretching of the charged jet during its flight to the target, (4) viscoelastic force which tries to prevent the charged jet from being stretched, (5) surface tension that also acts against the stretching of the surface of the charged jet, and (6) drag force from the friction between the charged jet and the surrounding air.[83] In the following section, practical factors influencing the morphology of nanofibers are explained regarding to their influence in sensitivity of gas SMO sensor.

Polymer concentration is an important operational parameter in the electrospinning process, which influence the fiber morphology significantly. The formation of the fibers is inhibited in the solutions with high concentrations due to their high viscosity.[84] The high viscosity makes the solutions difficult to flow through the syringe needle to form nanofibers under an electrostatic force.[85] Therefore, appropriate solution concentration becomes one of the key parameters to optimize the final electrospinning fibers. Extremely low solution viscosity can cause the formation of beads in nanofibers despite solutions with relatively high viscosity, in which the stable jets without breaking due to the cohesive nature of the high viscosity, travel to the electrode and form the uniform fibers on the collecting grounded electrode. Sol–gel electrospinning of metal oxides is based on the electrospinning of a solution of metal–organic precursors (alkoxides, chlorides, nitrates, acetates, or acetylacetonates) in a volatile solvent (alcohol, acetone, or water) and organic polymers (PVA, PVP, PEO, or PAN). The viscosity and conductive of the other *f* solution are increased evidently as the polymer concentration is increased[85] and by increasing the viscosity of the solution, the average diameters of the as-spun fibers decrease.[83] The choice of solution composition is based on the compatibility and solubility of a certain metal oxide precursor with a polymer solvent and the ability to achieve the required viscosity of the solution. Nevertheless, sometimes, a surfactant is needed to make the inorganic nanoparticles effectively disperse in the polymer.[7]

High-concentration results in elevated viscosity and surface tension, thereafter the stretching ability was reduced so the diameter of nanofibers would increase.[85–87] Moreover, the applied electrical voltage has an evident influence on fiber morphology. The surface tension of the solution and the electrostatic force should be balanced to obtain stable jets to form continuous fibers. Once the applied voltage exceeds the critical voltage, the jets of the liquids will get ejected from the cone tip. The jets will not be stable, which is responsible for the bead formation (sometimes called electrospray if the beads are separate particles) if the solution viscosity is extremely low. High voltage can generate more charges to the solution or droplet surface located at the tip of the needle (larger coulombic forces) as well as a stronger electrical field (larger electrostatic forces), both of which will stretch the jets fully for the favorable formation of the uniform and smooth fibers.[12,14] As it is shown in Fig. 5 nanofibers have beads in their structure and after annealing, they showed sensitivity towards NO gas, however, the influence of free-bead nanofibers is not studied on the sensitivity of NO gas. Fig. 5 demonstrates that NO detection was carried at 33 ppm which indicates the potential of detecting this gas in ppb level for disease diagnosis in the future.

The electric field strength is known to increase with the rise of the applied voltage. Yet, a critical voltage is required to obtain the cone for fiber formation even though the working distance is very small with very strong electric field strength. The unbalanced effect resulted that the prepared fiber exhibiting size distribution when high voltage was applied.[7] It has been pointed out that the feed rate of the polymer solution strongly influences the polymer fiber morphology.[9] There is an optimum for the feed rate and once the feed rate is sufficient enough to form fibers, a higher feed rate will supply more solution and is recognized as excess, which will produce fibers with beads.[84]

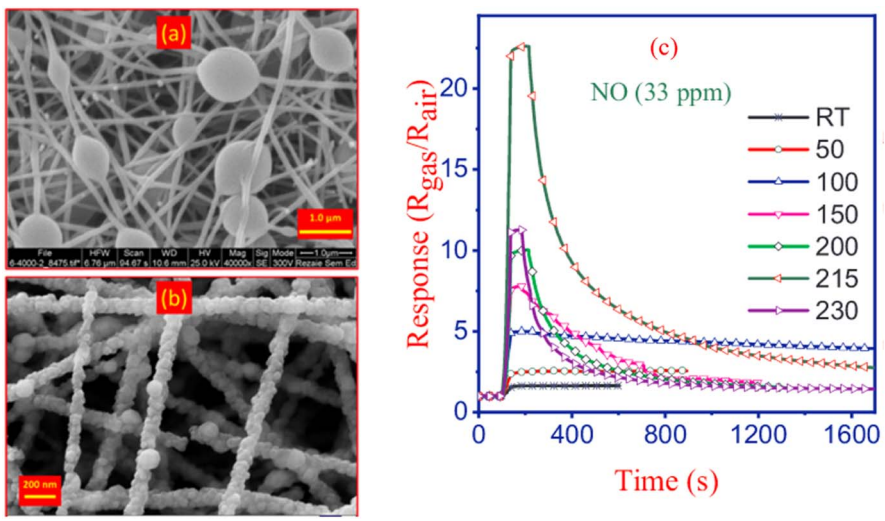

Fig. 5 Formation of beads in nanofibers prepared by electrospinning (a) before calcination, (b) FESEM image of ZnO/CdO nanofibers obtained after calcination, and (c) ZnO/CdO response to 33 ppm NO at different temperatures.[60] Reproduced from (ref. 60) with permission from Elsevier, copyright 2019.

Table 1 Electrospinning parameters of various SMO nanofibers in previous studies for NO and NO_2 detection

SMO	Polymer/solvent	Voltage (kV)	Feed rate	Distance (cm)	Calcination temperature, rate and duration	Diameter of nanofibers (before/after calcination)	Target gas concentration	Temperature (°C)	Response (R_g/R_a)	Ref.
ZnO	PVP/DMF	18	0.4 mL h^{-1}	20	500 °C, 4 h	200 nm	NO 50 ppb and 10 ppm	150 °C	1.04 and 36.17	92
Hollow SnO_2	PVP/DMF	14	0.3 mL h^{-1}	15	500 °C, 2, 6, and 10 °C min^{-1}, 2 h	Pore width: 2.22 to 26.52 nm	NO 500 ppb	100–200	0.1, 33.3, and 17.6	93
In–SnO_2	PVP/DMF	—	—	—	—	—	NO 100 ppm	—	737.8 $((R_g - 1/R_a) \times 100)$	94
Au-polyaniline/ZnO	PVA/distilled water	16	0.5 mL h^{-1}	14	600 °C, 2 h	400 nm	NO_2 10, 30, and 50 ppm	200–450	50 for 50 ppm	95
Bi-doped SnO_2	DMF/PVP	14	0.2 mL h^{-1}	15	600 °C/1.5 °C min^{-1}, 2 h	—	NO 217–10 ppm	75	217 for 10 ppm	96
ZnO/CdO	PVP/ethanol and DMF	18	0.4 mL h^{-1}	14	550 °C, 2 °C min^{-1}, 3 h	76–118 nm/70–100 nm	NO 3–33 ppm	200	10 to 22.6	60
WO_3 nanofibers with silver doping	PVA/distilled water	19	0.5 mL h^{-1}	15	500 °C, 1 °C min^{-1}, 2 h	103 ± 9 nm	NO_2 0.5–5 ppm	200–275	90.3 for 5 ppm at 225	89
Hollow ZnO	PVA/distilled water	10	0.5 mL h^{-1}	20	500 °C, 0.5 h	150 nm	NO_2 0.1, 1, 5, and 10 ppm	375	38 for 10 ppm	97
rGO nanosheets-loaded ZnO nanofibers	PVA/distilled water	15	0.3 mL h^{-1}	20	500 °C, 5 h	150 nm	NO_2 1–2–5 ppm	400	120 for 5 ppm	98
Al_2O_3–In_2O_3	DMF/PVP	15	0.25 mL h^{-1}	—	550 °C/1 °C min^{-1}, 4 h	Nanoparticles: 10 nm	97 ppm NO_x	Room temperature	100	91
PEDOT: PSS/TiO_2	PVP/ethanol	6	100 l h^{-1}	15	550 °C, 1 °C min^{-1}, 5 h	60–80 nm	NO 5 to 50 ppb	Room temperature-40% humidity	3 to 33	99
ZnO	—	—	—	—	—	—	NO 12 ppm	200 °C	7	100

Additionally, it is reported that the chance of fiber contraction (shrinkage) increases with the increase in the working distance.[15]

The fiber diameter is observed to decrease, and uniformity is to increase gradually with the increase of the working distance to reach an optimum point, after this point by increasing the distance the uniformity of the fibers drops and even some cracks are observed in the fibers.[13] Typically, lower number of fibers per area should be obtained when there was a larger distance between the tip of the nozzle and collector device since the stretched polymer deposited in a larger area and lower repetition of fiber deposition. Oblong beaded fibers were found when the distance was higher because the time interval was longer for polymer stretching. However, the increased distance did not solve the formation of beaded fibers prepared with electrospinning.[7,13]

In addition, the collection of nanofibers in the sensing area can be precisely controlled through the utilization of electrospinning technology. Notably, the implementation of near-field electrospinning has been achieved by reducing the distance between the collector and spinneret to a range of 500 μm to 5 cm. This unique approach eliminates the occurrence of bending instability, enabling the application of fibers with high spatial resolution. In a study by Zhang *et al.*,[88] they successfully reduced the deposition areas to 4, 2.8, and 1.7 cm^2 by minimizing the distance between the spinneret and the collector to 2.6, 2.1, and 1.7 cm, respectively. The average diameter of the WO_3 nanofibers after calcination was measured and found to be 103 ± 9 nm. The gas response for NO_2 is improved by Ag additives, so, they suggested increased surface activities of WO_3 materials with Ag additives.[89] In another study by Liao *et al.* the influence of ZnO diameter on sensing response was investigated, and the 100 nm sample exhibited the highest response.[90] Continuingly, Table 1 presents the electrospinning parameters employed for different semiconducting metal oxide nanofibers used in the detection of both NO and NO_2 gases. Different combinations of conditions lead to different nanofiber morphology, which reveals that electrospinning is a powerful method to synthesize desired 1D nanostructures.[91]

The preceding section delves into the intricate interplay of all four parameters, each of which exerts a discernible influence on the resultant nanofiber diameters. It is noteworthy that distinct configurations in the electrospinning parameters yield varying morphologies, which in turn contribute significantly to the ultimate sensitivity of the NO and NO_2 gas detection. Another pivotal factor in inducing morphological alterations is the calcination step. In accordance with the research conducted by Naderi *et al.*, their findings reveal that annealing at 400 °C yields a notably improved material response. This enhancement can be attributed to the heightened crystallinity achieved through this annealing temperature, thereby leading to more effectively sintered grains. Consequently, these optimized grain characteristics facilitate the seamless transfer of electrons across grain boundaries, thereby contributing to the material's enhanced performance.[60]

The Al_2O_3–In_2O_3 nanocomposite was able to detect NO_x gas at room temperature, which, of course, is high gas density and since this gas is required to be detected in lower concentrations.[91] Therefore, in other studies morphological parameters were investigated to enhanced the sensing performance because the size of nanograins, in addition to crystallinity and nanofiber diameter,[88] constitutes vital factors significantly influencing the electrical and sensing properties of oxide nanofibers. Nanofibers, consisting either of smaller grains or higher crystalline quality, usually show better-sensing properties than those either of larger grains or inferior crystalline quality.[97] This can be optimized in the calcination process. The combination of small grain size, high surface area, and high porosity that includes both small and large pores is ideally suited for gas sensing. Electrospinning followed by the calcination process results in highly porous structures that often display pore size distribution with relatively large pores (submicron to a few microns) between the fibers and nanosized pores within the fibers. This unique morphology facilitates easy penetration of the surrounding gas phase into the layer and effective distribution of the reactants to the surface of the metal oxide nanoparticles inside the layer. This probably shows high gas sensitivity in metal oxide gas sensors produced by electrospinning.[101] In Li *et al.*'s work,[41] different calcination condition reveals that ZnO based sensors showed its highest response (R_g/R_a) of 78.54 to 10 ppm of NO gas at calcinated temperature of 600 °C.

5 Reporting of sensing capabilities: strategies and outcomes in metal oxide nanofiber modification and post-modification processes

The blending method encompasses a process aimed at altering the characteristics of nanofibers by directly introducing modifying additives into the electrospinning solution. The concentration of the introduced dopant can be meticulously controlled and optimized to achieve optimal sensitivity. Post-modification involves the initial electrospinning preparation of metal oxide nanofibers, followed by subsequent treatments like noble metal incorporation, which influence the final properties of the formed nanofibers. Different structures can also be extended to the creation of hollow, porous and core–shell metal oxide architectures.[102] Critical factors influencing structure outcomes include the concentration of metal precursor within the solution, the resultant nanofiber diameter, and the interplay between the precursor solution and the ambient conditions during both electrospinning and subsequent calcination steps. Particularly, the interaction between various components at the interface of composite nanofibers synergistically influences gas-sensing performance. Additionally, incorporating porous structured nanofibers further improves the intrinsic high surface area, as expounded in studies.[103,104] The subsequent section of this article presents an extensive review of research studies focused on metal oxide materials, specifically ZnO, SnO_2, WO_3, and TiO_2. These materials are fabricated using the electrospinning technique and are explored for their efficacy in detecting both NO and NO_2 gases. The performance of the

sensor, particularly its sensitivity and working temperature, has been reviewed in relation to alterations in structural properties and composite materials.

5.1 ZnO nanofiber sensing layer

Zinc Oxide has been used extensively in the production of sensors as an interesting chemically and thermally stable n-type semiconductor with a large exciton binding energy and a wide band gap of 3.37 eV. Many investigations on sensors based on ZnO have been reported for the detection of toxic and combustible gases.[48,50] It is a promising gas-sensing material for its excellent gas-sensing response characteristics and long-term stability. Moreover, the improvement in the sensitivity and response speed of ZnO gas sensors can be achieved by nanostructure fabrication.[60] To explore the sensor performance of ZnO-based nanofibers, different composites and structure are studied through electrospinning. It is observed that the porous structure has higher response to the gas. Choi *et al.*[105] developed ZnO nanofiber-based NO_2 sensors and compared them to conventional thin-film ZnO-based gas sensors. They found that the response of nanofiber based NO_2 sensors at 350 °C was higher and faster, however, they did not mention recovery/response time in their study which needs to be investigated. Further investigation demonstrated that the response of ZnO nanofiber gas sensors can be increased by doping,[106,107] heterojunction fabrication,[108] and noble metal decoration.[106]

In the specific context of NO_2 gas detection, a study examined ZnO–SnO_2 hollow composite nanofibers with varying Zn ratios, leading to the synthesis of distinct materials evaluated for gas-sensing capabilities.[109] Demonstrating real-time sensing responses for ZnO–SnO_2 composites in Fig. 6 with varying Zn atom percentages at the optimal operating temperature of 90 °C reveals that the $SnZn_{20}$ sample achieves the highest response. This one-dimensional hollow nanostructure demonstrating a responsive behavior surpassing that of pristine ZnO and SnO_2 nanofibers by factors of 9 and 5.2, respectively. Importantly, this structure exhibited selectivity towards NO_2 over other gases, including ammonia, carbon monoxide, methanol, ethanol, and formaldehyde with response/recovery time of 68/83 s respectively. ZnO hollow fibers with smaller hole diameters were more sensitive to oxidizing gases than those with larger diameters. The improved gas-sensing ability was attributed to the increased surface area of the hollow fibers due to the smaller hole diameter.[97]

Later, in 2019, Naderi *et al.*,[60] applied the electrospinning method followed by calcination to synthesize ZnO/CdO nanofibers. They improved the ability of sensor to detect lower concentration of NO gas. In their study, an electroless gold-plated interdigitated electrode with a spacing of 200 μm is fabricated on an alumina substrate to host the designed nanofibers being used as gas sensors. The gas-sensing activity of the heterojunction is investigated against NO and analyzed by monitoring resistance changes. The ZnO/CdO nanofibers are found to be highly sensitive to a very low concentration range of NO gas (1.2–33 ppm) at other minimal operating temperatures of 215 °C. Additionally, repeatability and long-term stability (45 days, every 5 days, standard deviation = 0.7) were obtained for this sensor. Short response times of 47 and 35 seconds and recovery time of 1249 and 630 seconds are achieved *versus* 3 and 33 ppm of NO, respectively as it is shown in Fig. 6. This may be attributed to the energy band diagram of ZnO/CdO nanofibers as n–n heterojunction and their role in facilitating more electron transfer within the sensor and from the sensor to the NO gas molecules which is depicted in Fig. 7. In addition, CdO is known as an n-type semiconductor with a large number of native oxygen vacancies because of which it has low resistance.[20] Therefore, CdO decreases the resistance of the CdO/ZnO enabling the easy detection of the resistance variation during the sensing measurement and the rapid electron transportation between the electrodes of the sensor. The above-mentioned oxygen vacancies cause more adsorption of oxygen molecules on the surface of the CdO/ZnO heterojunction, which is beneficial to the surface reaction activity/kinetics, and thereby strengthens the sensing properties.[110] The selectivity of the sensor against NO could be attributed to the lower activation energy of the material against it, which accelerates its

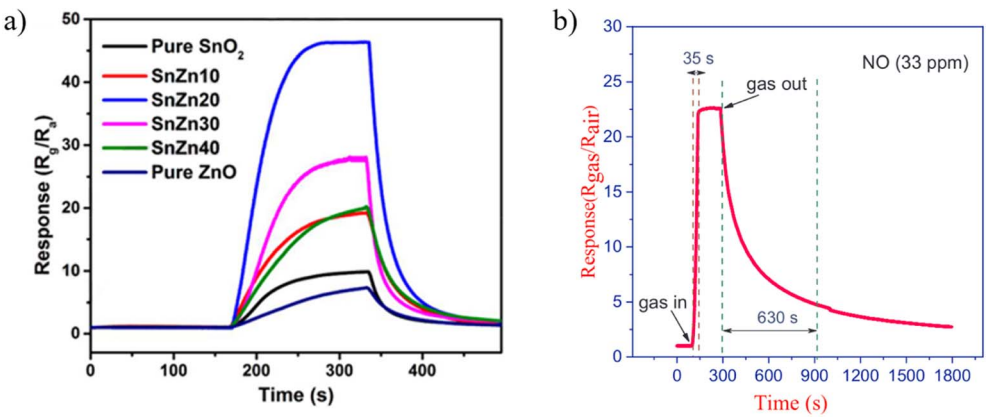

Fig. 6 The real-time sensing response for (a) ZnO–SnO_2 composites with different Zn atom percent at optimum operating temperature of 90 °C towards 1 ppm NO_2.[109] Reproduced from (ref. 109) with permission from Elsevier, copyright 2018. (b) ZnO/CdO nanofibers at 215 °C against 33 ppm of NO.[60] Reproduced from (ref. 60) with permission from Elsevier, copyright 2019.

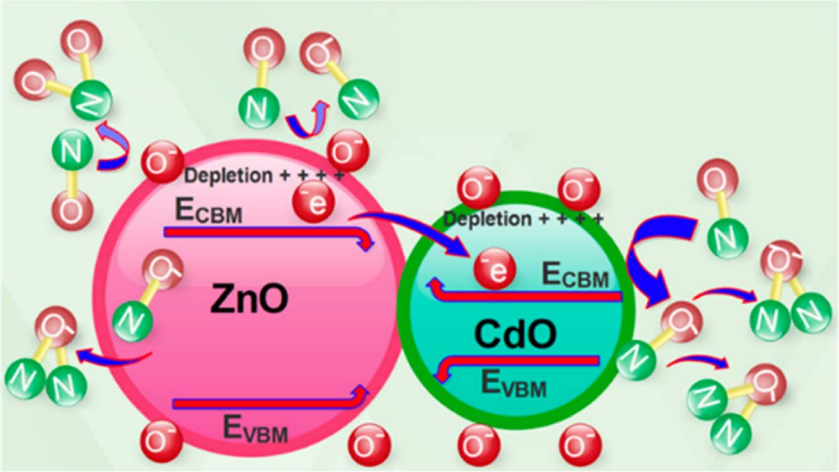

Fig. 7 The suggested mechanism of NO gas-sensing.[60] Reproduced from (ref. 60) with permission from Elsevier, copyright 2019.

desorption reactions and enhances the NO sensing performance compared to other gases/VOCs.

Regarding the influence of heterojunction, recently, Bonyani *et al.*, fabricated Au-decorated polyaniline (PANI)-ZnO by electrospinning for detecting NO_2 gas. The diameter of the ZnO nanofibers increased because of the presence of PANI. In addition, for the sample with 50 wt% PANI, many ZnO nanofibers are bonded together, which ultimately decreases the overall surface area of the ZnO nanofibers.[95] Au-decorated ZnO-NI (25 wt%) composite nanofiber gas sensor showed a response (R_g/R_a) of 50 towards 50 ppm NO_2 at 300 °C. The enhanced sensing response stemmed from the optimal amount of Au, generation of Au–ZnO Schottky junctions, and catalytic effect of Au NPs. Gold nanoparticles (Au NPs) play two significant roles in the gas sensing mechanism of Au-decorated ZnO nanofiber gas sensors. Firstly, Au acts as a catalyst, facilitating the dissociation of incoming O_2 gas molecules on its surface. This results in the efficient dissociation of oxygen molecules on the Au NP surface. Through a spillover effect, the ionic oxygen species then migrate to the adjacent ZnO surface, leading to enhanced reactions with NO_2 gas and consequently yielding a higher response. Secondly, due to the disparity in work functions between Au (>5.35 eV) and ZnO (5.2 eV), electrons transfer from ZnO to Au upon close contact, equalizing the Fermi levels and forming Schottky junctions.[38] Consequently, the presence of Au NPs results in an expanded width of the electron depletion layer compared to that of pristine ZnO nanofibers.

Further exploration of the performance of Au compositions enhanced by ZnO is warranted in various applications. Notably, Ponnuvelu *et al.*'s study addresses the impact of humidity by presenting insights into the sensing performance of Au-doped ZnO nanofibers. This particular set of sensors holds promise for environments characterized by high humidity levels, such as exhaled breath situations. In their study, heterojunction material showed an improved behavior at RH of 20% than at higher RH (90%). At higher RH% the formation of a moisture layer over the sensing film occurred and thereby resulting in reducing the physisorption process. The ZnO/Au heterojunction nanofibers exhibited a typical nanograined structure with 1D morphology consisting of two distinct lattice fringes corresponding to Au and ZnO and exhibited increased NO_2 gas-sensing properties when compared with ZnO nanofibers due to the electron transfer process between Au and ZnO at the interfaces and the presence of surface defects in the nanograins.[111]

To investigate the influence of additives on working temperature of sensors, Abideen *et al.*, produced ZnO nanofibers/reduced graphene oxide (rGO) *via* the electrospinning method.[98] They found out that rGO nanosheets do not affect the size of the ZnO nanograins or the diameter of nanofibers. NO_2 gas molecules adsorb onto the surfaces of the nanofibers, diffuse, take electrons from, and then create electron-depleted regions, eventually leading to a decrease in the conductivity of the nanofibers. Likewise, the emission of electrons occurs when the NO_2 gas is removed. However, the transfer of electrons and the formation of anions on the surface of the sensing material are significantly dependent on the temperature and sensing material. Sensors containing rGO showed a higher response than pure ZnO nanofibers at 300 °C, 350 °C, and 400 °C. It is noteworthy that the best response was achieved at 400 °C. To develop highly sensitive NO gas sensor Rh-doped ZnO nanofibers were prepared by electrospinning. At the optimal operating temperature of 150 °C, its response values (R_g/R_a) were 1.04 and 36.17, with the corresponding response time of 45 s and 32 s, towards 50 ppb and 10 ppm NO, respectively. The sensor also exhibits good selectivity, repeatability and linearity between the relative humidity and the response values. This way, the sensor was able to reduce working temperature and also response/recovery time.[92] Nonetheless, this structure needs to be studied more towards NO and NO_2 gases to decrease the working temperature of ZnO based nanofibers gas sensor and improve selectivity towards sensor array.

5.2 SnO_2 nanofiber sensing layer

Tin oxide is a highly studied metal oxide due to its remarkable stability, wide bandgap of 3.6 eV, and excellent electron

mobility. SnO_2-based metal oxide sensors typically require high operational temperatures for effective gas sensing, resulting in increased power consumption and reduced sensor lifespan. Nevertheless, this challenge can be effectively addressed by leveraging a different structure such as a core–shell, porous, hollow, and noble metals into the sensor design.[112] Reports show that hollow SnO_2 nanotubes exhibit maximum responses at a certain temperature with lower response/recovery time.[93,109] Therefore, dual factors, particularly, analyte and temperature, can strongly affect the sensing performance like response/recovery time.

Regarding decreasing the working temperature of SMOs gas sensors, in 2022, Su *et al.* obtained hollow electrospun SnO_2 nanotubes by controlling the ramping rate of calcination and investigating their sensing response to NO. During calcination, two opposite effects may occur, leading to the formation of different morphologies. The first effect is the shrinkage of nanofibers because of the decomposition of PVP during heating, which forms solid nanotubes. The other is the diffusion of gases (primarily originating from PVP decomposition) from the inside of nanofibers toward the outside of nanofibers, which causes the expansion of nanofibers, thereby forming hollow nanotubes. When the heating rate is slow (*e.g.*, 2 °C min^{-1}), the diffusion rate of gases through the interspace among SnO_2 nanoparticles is faster than the decomposition rate of PVP. They found out that a low heating rate (2 °C min^{-1}) results in the formation of solid SnO_2 nanotubes, while a high heating rate (10 °C min^{-1}) makes most nanotubes collapse as it is shown in Fig. 8a. The medium heating rate (6 °C min^{-1}) can construct hollow SnO_2 nanotubes. In comparison with solid SnO_2 nanotubes, hollow SnO_2 nanotubes possess higher surface area and more abundant oxygen species, which is favorable for the sensing performance, especially the sensitivity. Considering different humidity, hollow SnO_2 nanotubes in Fig. 8b exhibits a high sensitivity of 33.3 toward 500 ppb NO and can detect NO down to 10 ppb at low temperature of 160 °C. Upon exposure to 500 ppb of NO, the response time is 214 s, and the recovery time is 115 s. As the gas concentration increases, the response time and recovery time shorten. However, there is a lack of comprehensive understanding of the relationship between the structure and the sensing performance.[93]

In another study, Su *et al.*,[93] demonstrated that hollow SnO_2 nanotubes (NTs) exhibited a remarkable sensing performance for NO at 160 °C. The sensing materials were prepared by direct annealing of electrospun precursor nanofibers, and hollow NTs can be obtained at an appropriate heating rate of 6 °C min^{-1}. Given the large surface area of hollow SnO_2 NTs, their sensing performance is better than that of solid SnO_2 NTs. The response of hollow SnO_2 is approximately 33.3 upon exposure to 500 ppb of NO at 160 °C.

In an effort to diminish the operating temperature of sensors, with consideration for the structure of the electrospun composition, Bai *et al.* evaluated the potential of the SnO_2–ZnO core–shell nanofiber to detect NO_2.[109] At an operating temperature of 90 °C, the SnO_2–ZnO composite-based sensors demonstrate a response of approximately 5.2 which is 9 times greater than that of pure SnO_2 and ZnO sensors, respectively. Thereafter, to decrease the working temperature of sensors, in 2021, Ma *et al.*[96] demonstrated the highly sensitive and selective detection of NO by Bi-doped SnO_2 two-dimensional ultrathin nanosheets with porous structures, fabricated using electrospinning method. In this study, SnO_2 with 0.75 mol% bismuth (Bi) detects 10 ppm of NO at a relatively low temperature of 75 °C with a response of 217. Further, a low detection limit of 50 ppb has also been achieved, however, the response/recovery time is not reported in their study. They indicated that sensing properties can be attributed to the ultrathin structure, which has a high surface area and abundant pores.

Noble metal doping or decoration may diminish some gas sensing performance and it depends on the gas analyte. Jang *et al.* fabricated gas sensors based on Pt nanoparticles functionalized SnO_2 nanofibers.[113] Varying the concentrations of Pt

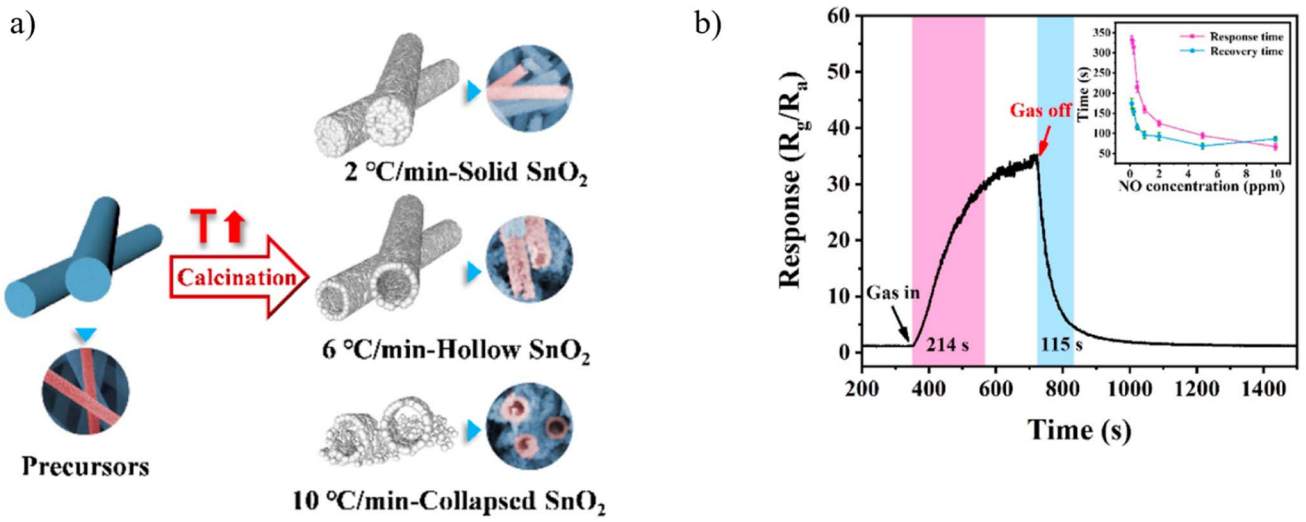

Fig. 8 (a) Schematic representation of hollow nanofibers obtained from calcinated electrospun nanofiber (b) dynamic response curves of the sensors towards 500 ppb NO gas at 160 °C under 20% RH.[93] Reproduced from (ref. 93) with permission from Elsevier, copyright 2022.

nanoparticles, the authors showed that the sensitivity to NO_2 decreased with the introduction of Pt nanoparticles in SnO_2. In this case, with Pt functionalization, upon exposure to oxidizing agents, the additional electron trapping is smaller than that of pristine SnO_2 nanofibers leading to a lower sensitivity to NO_2. Calculating the absorbed energy and charge transfer with various dopants enables researchers to find the best dopant for a specific analyte.[114]

5.3 WO_3 nanofiber sensing layer

Tungsten trioxide with an energy band gap of 2.6 to 3.0 eV is a metal oxide semiconductor that is structurally polymorphic, meaning that it has a wide variety of structural forms that depend on several parameters. A nanostructured chemiresistor based on a polymorphic WO_3 was used to selectively detect the low concentration of NO.[115] The parameters that are most likely to affect its structure are the heating/annealing treatment in the synthesis stage, and also the additives in the oxide. Basically, according to Bonardo *et al.* WO_3 showed a perovskite-like cubic structure based on the angular division of a regular octahedron with an oxygen atom in each corner and a tungsten atom at the center. Several researchers in the production of WO_3 have resulted in three common crystal structures, namely monoclinic, orthorhombic, and hexagonal.[52] In this regard, Zhang *et al.*[116] developed WO_3 nanofiber-based NO_2 sensors and compared them to conventional thin-film WO_3-based gas sensors by changing the heating rate of calcination step. Their sensor displayed response of 101.3 as it is shown in Fig. 9 and the response time (125 s)/recovery time (231 s) toward 3 ppm NO_2 at 90 °C. Diffusion coefficient and strong absorbing capability for surface species and NO_2 gas molecules, originating from the high porosity, high oxygen vacancy concentration, and high surface area. An alternative strategy for enhancing sensor performance involves is using various types of carbon nanotubes such as graphite, graphene, reduced graphene oxide, carbon dots, and carbon nanotubes as the second phase in WO_3-based gas sensors.

The exceptional attributes of these carbon materials significantly contribute to enhancing sensing performance.[117] rGO,

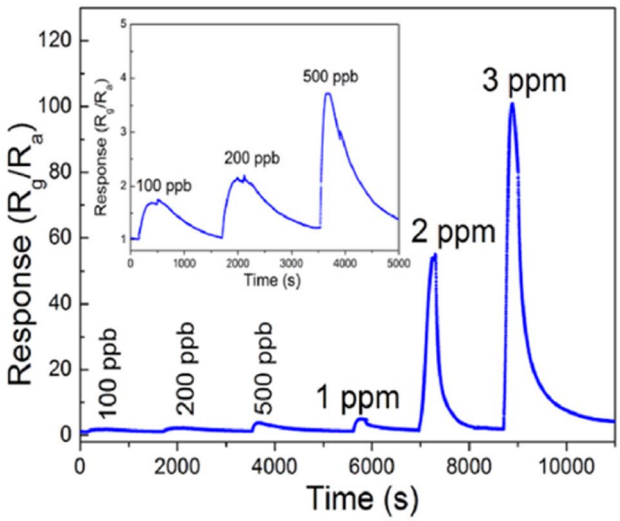

Fig. 9 Response curves of the WO_3 nanofiber-based sensors to various NO_2 concentrations at 90 °C.[116] Reproduced from[116] with permission from Elsevier, copyright 2021.

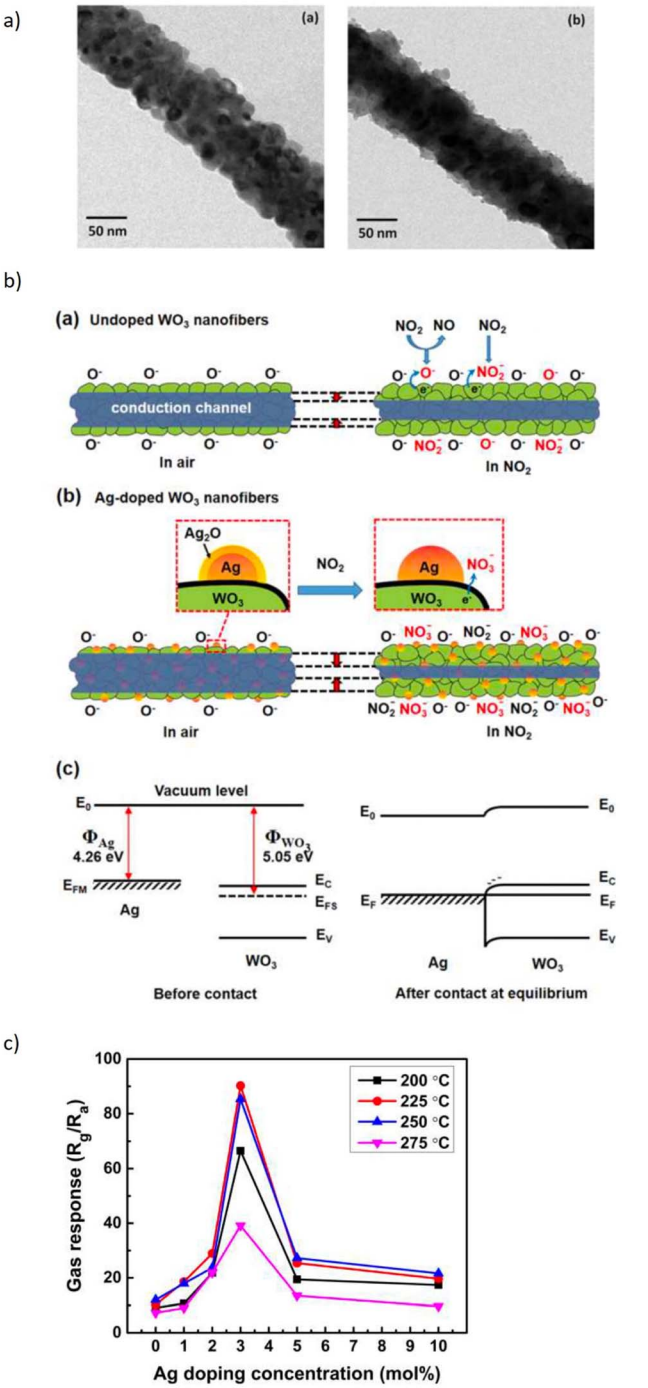

Fig. 10 (a) TEM micrographs of the resulting (a) Ag-doped and (b) undoped WO_3 nanofibers and, (b) schematic of sensing NO_2 in (a) undoped (b) Ag-doped and (c) energy level before and after injection of gas, (c) gas response plot of the WO_3 nanofiber gas sensors with various Ag doing concentrations. The sensors were exposed to 5 ppm NO_2 at different operating temperatures.[89] Reproduced from (ref. 89) with permission from Elsevier, copyright 2018.

which is a p-type semiconductor, will form a p–n junction with WO_3, which is an n-type semiconductor. In addition to augmenting the response signal towards gas targets, the inclusion of rGO in WO_3-based sensors also has the potential to lower the operational temperature of the sensor. Concerning noble metals, Yoo *et al.* showcased that Pt-WO_3 exhibits remarkable sensitivity to NO. Nevertheless, the hydrothermal synthesis method employed for its creation imposes constraints on its scalability and versatility. Consequently, there arises a compelling need to investigate the potential of electrospinning—an alternative technique offering enhanced scalability and versatility—for synthesizing Pt-WO_3. By investigating the electrospinning technique, we can assess its efficacy in producing Pt-WO_3 with enhanced properties and evaluate its suitability for large-scale production of highly sensitive nitric oxide sensors.[118]

The effects of noble metal dopants on the performance of various types of sensors have been the subject of studies. Jaroenapibal *et al.*[89] fabricated Ag-doped WO_3 nanofiber-based gas sensors using an electrospinning technique. In the electrospinning setup, the DC power supply was set to 19 kV and the distance between the needle and the metal collector was 15 cm. The solution was electrospun at the rate of 0.5 mL h^{-1}, resulting in the deposition of nanofibers onto the electrodes. To control the density of the nanofibers on each substrate, exactly 1 mL of solution was ejected from the syringe. Transmission electron microscopy (TEM) images showed a form of nanofiber in Fig. 10a. As expected, the Ag-doped WO_3 nanofibers showed an improved performance for NO_2 sensing when compared with pristine WO_3. It was observed that at 0.5 ppm NO_2 concentration, the gas response of 7.7 was exhibited. The proposed mechanism suggested the electron injection from Ag to WO_3, expanding the depletion layer compared to pristine WO_3, as it is demonstrated in Fig. 10b. Since NO_2 is an oxidizing gas when in contact with Ag-doped WO_3 nanofibers, it will improve the depletion layer modulation (Fig. 10b). Besides, the additional Ag_2O also contributes as a chemical sensitizer when in the presence of NO_2. The response of doped electrospun SMOs with noble metals is attributed to both electronic and chemical modulation of the material. Fig. 10c underlines the effect of Ag dopant concentration on the gas response of WO_3 nanofiber gas sensors. The gas response was observed to peak for the sample with an Ag dopant concentration of 3 mol%. This may be due to the fact that this dopant level allows the most effective dispersion of small Ag nanoparticles throughout WO_3 grains.

5.4 TiO_2 nanofiber sensing layer

Titanium dioxide is a high resistance n-type semiconductor material with a band gap of around 3 eV, has attracted significant attention for its applications in gas sensors due to its environmental friendliness, chemical stability, catalytic properties, and the modulation in its structural, optical, and transport properties. Additionally, TiO_2 has a three-crystal structure in nature: anatase, brookite, and rutile. Rutile is the most stable while the anatase and brookite phases are metastable and can be converted irreversibly to the rutile phase when heated under high temperatures in the range of 600–800 °C. Anatase is the most widely gas sensor due to its prominent gas reaction capacity and high oxygen vacancies.[1]

As working temperature is a weakness of SMOs, in Moon *et al.*'s work,[119] Pd-doped TiO_2 fibers have demonstrated auspicious attributes for gas sensing applications, notably encompassing a notably low operational temperature of 180 °C, coupled with a commendable gas response (characterized by R_g/R_a values ranging from 38 to 2.1 at a NO_2 concentration of 2.1 ppm). The methodologies expounded herein introduce novel avenues for the fabrication of metal-oxide nanofibers infused with catalytic dopants, thereby advancing the realm of gas-sensing technologies. Then, in 2021, room temperature-based NO gas sensor of TiO_2-rGO composite nanofibers was prepared using electrospinning and solvothermal synthesis by Kuchi *et al.*.[120] They demonstrated that when the composite was exposed to the NO gas, it exhibits gas sensing property at 30 °C. This composite sensor sensitivity is 7.1 when exposed to 2.75 ppm of NO gas 440 seconds response time. This study underscores the potential applications of TiO_2-rGO composite nanofibers in the realm of gas sensing, particularly for the detection of low-concentration NO at room temperature.[60,61]

It is discussed in studies that a doping effect on the polymer by SMO-like TiO_2 nanostructures is capable to decrease the energy gap and increase the charge carriers available,[121] thus, lead to an increase in gas response in NO_x detection. Therefore, In Zampetti *et al.*'s study,[99] a hybrid electrospun nanofibrous framework of titania, generated at first by growing up the nanofibers directly onto an interdigitated electrode (IDE) as a transducer and then coating them with an ultra-thin film of PEDOT-PSS, was investigated as a potential sensing material for NO. Fig. 11 shows fine, rough and bead-free nanofibers and it

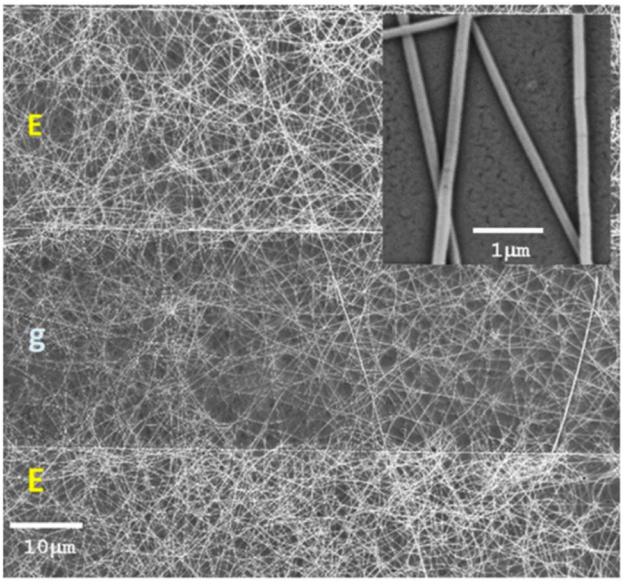

Fig. 11 SEM micrographs (mag: 1.41k×, 5 kV) of a 20 min TiO_2 electrospun fibrous layer coating the Pt/Ti electrodes (E) of an IDE after annealing in air, with a zoom-in (the inset) of a few fibers of ~80 nm mean diameter (mag: 34.40k×, 5 kV). The gap between two electrodes is specified with *g*.[99] Reproduced from (ref. 99) with permission from Elsevier, copyright 2013.

seems there is a proper combination of the electrospinning set of parameters, such as viscosity, chemical nature of solvents, molecular weight, and structure of the carrier polymer, nozzle-ground distance, potential applied, *etc.* NO measurements were performed by introducing the gas at increasing concentrations ranging from 5 to 50 ppb. It is important to note that NO concentrations below 1 ppm can be oxidized to NO_2 through stoichiometric reactions when appropriately humidified.[122] The sensor exhibited a response of approximately 1.05 towards 20 ppb of NO_x, however, the response time ranged between 5 and 17 min which is higher than the other studies.

6 Perspectives and future directions

The preceding sections provide a comprehensive overview of the multifaceted aspects surrounding semiconductor metal oxide electrospun nanofibers used as gas sensors for detecting NO and NO_2. The discourse encapsulates the structural design, fabrication process, performance evaluation, and compositional attributes of these sensors. One of the primary focal points of this review lies in delineating the intricate interplay between various electrospinning parameters, the resultant material structures, and compositions, as well as their collective influence on the sensitivity exhibited towards the two target gases.

This analysis underscores the imminent trajectories that future research endeavors within this domain are likely to pursue, with particular emphasis on two pivotal directions. Firstly, the quest to reduce gas detection limits through innovative designs and novel structures is anticipated to be a compelling avenue. This entails leveraging the principles of nanoscale engineering to refine sensing films, thus achieving heightened sensitivity and lowering detection thresholds to low ppb range. Detection limit of NO gas is a challenge for diagnostic application, that is why, up to now there are no practical SMO sensors available for detecting NO at low ranges.[6,25,123,124]

Significantly, considerable strides in this arena have arisen from advancements in fabrication techniques that offer improved control over nanoparticle characteristics. Secondly, the endeavor to augment the selectivity and precision of these sensors to bolster accuracy even under elevated humidity conditions emerges as a paramount goal. Achieving this objective in low temperatures involves a deep understanding of material selection, particularly its surface reactivity, which greatly influences selectivity. While the field has witnessed notable progress in creating selective interactions between metal oxides and specific analytes, the broader landscape of applied sensing materials often presents challenges in this aspect. However, potential avenues for enhancing selectivity are observed within SMOs with distinct compositions, metastable phases, solid solutions, mixed oxides, and heterojunctions, all of which contribute to the material's distinctive response. It's imperative to underscore that, when evaluating the sensitivity and detection limits of emerging sensing materials for applications such as breath analysis, assessments must be conducted under breath-realistic conditions. This entails simulating high relative humidity levels and relevant analyte concentrations within gas mixtures. This consideration ensures the practicality and reliability of sensor performance under real-world scenarios.

Looking forward, the convergence of advanced sensing fabrication methodologies, particularly utilizing electrospinning technology, holds great promise in discovering novel gas-sensitive materials that exhibit multifunctional attributes. These attributes encompass unique structural, electrical, and physical characteristics that synergistically enhance sensor performance. The versatility of electrospinning allows for the creation of solid, hollow, and core–shell fibers, with precisely controlled structures and compositions, thereby presenting remarkable opportunities for innovation and advancement in the realm of next-generation gas sensors to detect critical gases such as NO and NO_2.

Author contributions

Niloufar Khomarloo: writing – original draft preparation; Elham Mohsenzadeh, Hayriye Gidik, Roohollah Bagherzadeh: writing – review and editing; Masoud Latifi: supervision.

Conflicts of interest

The authors declare that they have no known competing financial interests or personal relationships that could have appeared to influence the work reported in this article.

References

1 F. Vajhadin, M. Mazloum-Ardakani and A. Amini, Metal oxide-based gas sensors for the detection of exhaled breath markers, *Med. Devices Sens.*, 2021, **4**(1), e10161.
2 K. Wetchakun, *et al.*, Semiconducting metal oxides as sensors for environmentally hazardous gases, *Sens. Actuators, B*, 2011, **160**(1), 580–591.
3 L. A. Mercante, R. S. Andre, L. H. Mattoso and D. S. Correa, Electrospun ceramic nanofibers and hybrid-nanofiber composites for gas sensing, *ACS Appl. Nano Mater.*, 2019, **2**(7), 4026–4042.
4 X. Chen and S. S. Mao, Titanium dioxide nanomaterials: synthesis, properties, modifications, and applications, *Chem. Rev.*, 2007, **107**(7), 2891–2959.
5 Z. Li, *et al.*, Advances in designs and mechanisms of semiconducting metal oxide nanostructures for high-precision gas sensors operated at room temperature, *Mater. Horiz.*, 2019, **6**(3), 470–506.
6 C. Sánchez, J. P. Santos and J. Lozano, Use of electronic noses for diagnosis of digestive and respiratory diseases through the breath, *Biosensors*, 2019, **9**(1), 35.
7 G. Korotcenkov, Electrospun metal oxide nanofibers and their conductometric gas sensor application. Part 1: Nanofibers and features of their forming, *Nanomaterials*, 2021, **11**(6), 1544.
8 X. Chen, G. Li, G. Zhang, K. Hou, H. Pan and M. Du, Self-assembly of palladium nanoparticles on functional TiO_2

nanotubes for a nonenzymatic glucose sensor, *Mater. Sci. Eng. C*, 2016, **62**, 323–328.
9 S. M. Lin, S. Geng, N. Li, N. B. Li and H. Q. Luo, D-penicillamine-templated copper nanoparticles *via* ascorbic acid reduction as a mercury ion sensor, *Talanta*, 2016, **151**, 106–113.
10 Z. Wang, *et al.*, High-performance reduced graphene oxide-based room-temperature NO_2 sensors: A combined surface modification of SnO_2 nanoparticles and nitrogen doping approach, *Sens. Actuators, B*, 2017, **242**, 269–279.
11 S. Zhang, Z. Jia, T. Liu, G. Wei and Z. Su, Electrospinning Nanoparticles-Based Materials Interfaces for Sensor Applications, *Sensors*, 2019, **19**(18), 3977. [Online]. Available: **https://www.mdpi.com/1424-8220/19/18/3977**.
12 A. Dey, Semiconductor metal oxide gas sensors: A review, *Mater. Sci. Eng. B*, 2018, **229**, 206–217.
13 M. Righettoni, A. Tricoli and S. E. Pratsinis, Si: WO3 sensors for highly selective detection of acetone for easy diagnosis of diabetes by breath analysis, *Anal. Chem.*, 2010, **82**(9), 3581–3587.
14 T. Akamatsu, T. Itoh, N. Izu and W. Shin, NO and NO_2 sensing properties of WO_3 and Co_3O_4 based gas sensors, *Sensors*, 2013, **13**(9), 12467–12481.
15 A. Macagnano, A. Bearzotti, F. De Cesare and E. Zampetti, Sensing asthma with portable devices equipped with ultrasensitive sensors based on electrospun nanomaterials, *Electroanalysis*, 2014, **26**(6), 1419–1429.
16 New Jersey Department of Health and Senior Service, *Hazardous Substance Fact Sheet: Nitrogen Dioxide*, 1989.
17 A. Ray, M. Raundhal, T. B. Oriss, P. Ray and S. E. Wenzel, Current concepts of severe asthma, *J. Clin. Invest.*, 2016, **126**(7), 2394–2403.
18 K. F. Chung, Personalised medicine in asthma: time for action: Number 1 in the Series Personalised medicine in respiratory diseases Edited by Renaud Louis and Nicolas Roche, *European Respiratory Review*, 2017, **26**, 145.
19 M. L. Levy, *et al.*, Key recommendations for primary care from the 2022 Global Initiative for Asthma (GINA) update, *NPJ Prim. Care Respir. Med.*, 2023, **33**(1), 7.
20 L. Bjermer, *et al.*, Current evidence and future research needs for FeNO measurement in respiratory diseases, *Respir. Med.*, 2014, **108**(6), 830–841.
21 T. H. Eom, *et al.*, Substantially improved room temperature NO_2 sensing in 2-dimensional SnS_2 nanoflowers enabled by visible light illumination, *J. Mater. Chem. A*, 2021, **9**(18), 11168–11178.
22 M. Huang, *et al.*, Synthesis of Cu_2O-modified reduced graphene oxide for NO_2 sensors, *Sensors*, 2021, **21**(6), 1958.
23 X. Yao, *et al.*, Flower-like hydroxyfluoride-sensing platform toward NO_2 detection, *ACS Appl. Mater. Interfaces*, 2021, **13**(22), 26278–26287.
24 Q. Li, W. Zeng and Y. Li, Metal oxide gas sensors for detecting NO_2 in industrial exhaust gas: Recent developments, *Sens. Actuators, B*, 2022, **359**, 131579.
25 T. L. Mathew, P. Pownraj, S. Abdulla and B. Pullithadathil, Technologies for clinical diagnosis using expired human breath analysis, *Diagnostics*, 2015, **5**(1), 27–60.
26 A. M. Fitzpatrick, Biomarkers of asthma and allergic airway diseases, *Ann. Allergy, Asthma, Immunol.*, 2015, **115**(5), 335–340.
27 R. A. Dweik and A. Amann, Exhaled breath analysis: the new frontier in medical testing, *J. Breath Res.*, 2008, **2**(3), 030301.
28 S. K. Medrek, A. D. Parulekar and N. A. Hanania, Predictive biomarkers for asthma therapy, *Curr. Allergy Asthma Rep.*, 2017, **17**, 1–13.
29 W. Wang, *et al.*, Zinc oxide nanofiber gas sensors *via* electrospinning, *J. Am. Ceram. Soc.*, 2008, **91**(11), 3817–3819.
30 Q. A. Drmosh, I. Olanrewaju Alade, M. Qamar and S. Akbar, Zinc Oxide-Based Acetone Gas Sensors for Breath Analysis: A Review, *Chem.–Asian J.*, 2021, **16**(12), 1519–1538.
31 S. Kischkel, *et al.*, Breath biomarkers for lung cancer detection and assessment of smoking related effects—confounding variables, influence of normalization and statistical algorithms, *Clin. Chim. Acta*, 2010, **411**(21–22), 1637–1644.
32 P. Paredi, S. A. Kharitonov and P. J. Barnes, Elevation of exhaled ethane concentration in asthma, *Am. J. Respir. Crit. Care Med.*, 2000, **162**(4), 1450–1454.
33 M. Barker, *et al.*, Volatile organic compounds in the exhaled breath of young patients with cystic fibrosis, *Eur. Respir. J.*, 2006, **27**(5), 929–936.
34 D. Hashoul and H. Haick, Sensors for detecting pulmonary diseases from exhaled breath, *European Respiratory Review*, 2019, **28**, 152.
35 M. Kaloumenou, E. Skotadis, N. Lagopati, E. Efstathopoulos and D. Tsoukalas, Breath Analysis: A Promising Tool for Disease Diagnosis—The Role of Sensors, *Sensors*, 2022, **22**(3), 1238.
36 H. Haick, Y. Y. Broza, P. Mochalski, V. Ruzsanyi and A. Amann, Assessment, origin, and implementation of breath volatile cancer markers, *Chem. Soc. Rev.*, 2014, **43**(5), 1423–1449.
37 A. Tiotiu, Biomarkers in asthma: state of the art, *Asthma research and practice*, 2018, **4**(1), 1–10.
38 F. Gu, R. Nie, D. Han and Z. Wang, In_2O_3-graphene nanocomposite based gas sensor for selective detection of NO_2 at room temperature, *Sens. Actuators, B*, 2015, **219**, 94–99.
39 A. Bikov, Z. Lázár and I. Horvath, Established methodological issues in electronic nose research: how far are we from using these instruments in clinical settings of breath analysis?, *J. Breath Res.*, 2015, **9**(3), 034001.
40 V. S. Bhati, M. Kumar and R. Banerjee, Gas sensing performance of 2D nanomaterials/metal oxide nanocomposites: A review, *J. Mater. Chem. C*, 2021, **9**(28), 8776–8808.
41 C. Li, *et al.*, Biomass-derived hierarchical porous ZnO microtubules for highly selective detection of ppb-level nitric oxide at low temperature, *Sens. Actuators, B*, 2021, **333**, 129627.
42 S.-C. Wang, *et al.*, NiO nanoparticles-decorated ZnO hierarchical structures for isopropanol gas sensing, *Rare Met.*, 2022, 1–12.

43 H. T. Hien, P. Q. Ngan, G. H. Thai, T. Trung, M. M. Tan and H. T. Giang, High NH3 sensing performance of NiO/PPy hybrid nanostructures, *Sens. Actuators, B*, 2021, **340**, 129986.
44 Shailja, K. J. Singh and R. C. Singh, Highly sensitive and selective ethanol gas sensor based on Ga-doped NiO nanoparticles, *J. Mater. Sci.: Mater. Electron.*, 2021, **32**, 11274–11290.
45 S. Zhang, B. Zhang, B. Zhang, Y. Wang, H. Bala and Z. Zhang, Structural evolution of NiO from porous nanorods to coral-like nanochains with enhanced methane sensing performance, *Sens. Actuators, B*, 2021, **334**, 129645.
46 M. S. Choi, *et al.*, Selective, sensitive, and stable NO_2 gas sensor based on porous ZnO nanosheets, *Appl. Surf. Sci.*, 2021, **568**, 150910.
47 J. Li, *et al.*, Fast detection of NO_2 by porous SnO_2 nanotoast sensor at low temperature, *J. Hazard. Mater.*, 2021, **419**, 126414.
48 H. Wang, *et al.*, The influence of different ZnO nanostructures on NO_2 sensing performance, *Sens. Actuators, B*, 2021, **329**, 129145.
49 A. Nanda, V. Singh, R. K. Jha, J. Sinha, S. Avasthi and N. Bhat, Growth-temperature dependent unpassivated oxygen bonds determine the gas sensing abilities of chemical vapor deposition-grown CuO thin films, *ACS Appl. Mater. Interfaces*, 2021, **13**(18), 21936–21943.
50 S. Park, Y. Byoun, H. Kang, Y.-J. Song and S.-W. Choi, ZnO nanocluster-functionalized single-walled carbon nanotubes synthesized by microwave irradiation for highly sensitive NO_2 detection at room temperature, *ACS Omega*, 2019, **4**(6), 10677–10686.
51 B. Yang, N. V. Myung and T. T. Tran, 1D metal oxide semiconductor materials for chemiresistive gas sensors: a review, *Adv. Electron. Mater.*, 2021, **7**(9), 2100271.
52 D. Bonardo, N. L. W. Septiani, F. Amri, S. Humaidi and B. Yuliarto, recent development of WO3 for toxic gas sensors applications, *J. Electrochem. Soc.*, 2021, **168**(10), 107502.
53 S. M. Majhi, A. Mirzaei, H. W. Kim and S. S. Kim, Reduced graphene oxide (rGO)-loaded metal-oxide nanofiber gas sensors: An overview, *Sensors*, 2021, **21**(4), 1352.
54 F. Sarf, Metal oxide gas sensors by nanostructures, *Gas Sensors*, 2020, vol. 1, pp. 1–17.
55 Z. U. Abideen, *et al.*, Electrospun metal oxide composite nanofibers gas sensors: A review, *J. Korean Ceram. Soc.*, 2017, **54**(5), 366–379.
56 Z. Hosseini and A. Mortezaali, Room temperature H_2S gas sensor based on rather aligned ZnO nanorods with flower-like structures, *Sens. Actuators, B*, 2015, **207**, 865–871.
57 J. Liu, *et al.*, Size effect and comprehensive mathematical model for gas-sensing mechanism of SnO_2 thin film gas sensors, *J. Alloys Compd.*, 2022, **898**, 162875.
58 Fitriana, N. L. W. Septiani, D. R. Adhika, A. G. Saputro, Nugraha and B. Yuliarto, Enhanced NO Gas Performance of (002)-Oriented Zinc Oxide Nanostructure Thin Films, *IEEE Access*, 2019, **7**, 155446–155454, DOI: **10.1109/ACCESS.2019.2949463**.
59 X. Zhou, *et al.*, Nanomaterial-based gas sensors used for breath diagnosis, *J. Mater. Chem. B*, 2020, **8**(16), 3231–3248.
60 H. Naderi, S. Hajati, M. Ghaedi and J. Espinos, Highly selective few-ppm NO gas-sensing based on necklace-like nanofibers of ZnO/CdO nn type I heterojunction, *Sens. Actuators, B*, 2019, **297**, 126774.
61 A. Nasriddinov, *et al.*, Effect of humidity on light-activated NO and NO_2 gas sensing by hybrid materials, *Nanomaterials*, 2020, **10**(5), 915.
62 K. Arun, M. Lekshmi and K. Suja, Performance analysis, modeling, and development of a signal conditioning unit of n-type metal oxide gas sensor for acetone gas detection, *J. Comput. Electron.*, 2021, **20**, 1938–1947.
63 E. Comini, Metal oxide nanowire chemical sensors: innovation and quality of life, *Mater. Today*, 2016, **19**(10), 559–567.
64 T. Zhang, S. Mubeen, N. V. Myung and M. A. Deshusses, Recent progress in carbon nanotube-based gas sensors, *Nanotechnology*, 2008, **19**(33), 332001.
65 H. Ji, W. Zeng and Y. Li, Gas sensing mechanisms of metal oxide semiconductors: a focus review, *Nanoscale*, 2019, **11**(47), 22664–22684.
66 W. Han, G. S. Bhat and X. Wang, Investigation of nanofiber breakup in the melt-blowing process, *Ind. Eng. Chem. Res.*, 2016, **55**(11), 3150–3156.
67 E. S. Medeiros, G. M. Glenn, A. P. Klamczynski, W. J. Orts and L. H. Mattoso, Solution blow spinning: A new method to produce micro-and nanofibers from polymer solutions, *J. Appl. Polym. Sci.*, 2009, **113**(4), 2322–2330.
68 S.-H. Yu, M. Antonietti, H. Cölfen and J. Hartmann, Growth and self-assembly of BaCrO4 and BaSO4 nanofibers toward hierarchical and repetitive superstructures by polymer-controlled mineralization reactions, *Nano Lett.*, 2003, **3**(3), 379–382.
69 V. A. Agubra, L. Zuniga, D. Flores, H. Campos, J. Villarreal and M. Alcoutlabi, A comparative study on the performance of binary SnO_2/NiO/C and Sn/C composite nanofibers as alternative anode materials for lithium ion batteries, *Electrochim. Acta*, 2017, **224**, 608–621.
70 Y. Dai, W. Liu, E. Formo, Y. Sun and Y. Xia, Ceramic nanofibers fabricated by electrospinning and their applications in catalysis, environmental science, and energy technology, *Polym. Adv. Technol.*, 2011, **22**(3), 326–338, DOI: **10.1002/pat.1839**.
71 X. Lu, C. Wang and Y. Wei, One-dimensional composite nanomaterials: Synthesis by electrospinning and their applications, *Small*, 2009, **5**(21), 2349–2370.
72 J. Xue, T. Wu, Y. Dai and Y. Xia, Electrospinning and electrospun nanofibers: Methods, materials, and applications, *Chem. Rev.*, 2019, **119**(8), 5298–5415.
73 Z. U. Abideen, J.-H. Kim, A. Mirzaei, H. W. Kim and S. S. Kim, Sensing behavior to ppm-level gases and synergistic sensing mechanism in metal-functionalized rGO-loaded ZnO nanofibers, *Sens. Actuators, B*, 2018, **255**, 1884–1896.

74 M. Imran, N. Motta and M. Shafiei, Electrospun one-dimensional nanostructures: a new horizon for gas sensing materials, *Beilstein J. Nanotechnol.*, 2018, **9**(1), 2128–2170.
75 S. J. Choi, *et al.*, Electrospun nanostructures for high performance chemiresistive and optical sensors, *Macromol. Mater. Eng.*, 2017, **302**(8), 1600569.
76 X. Wang, C. Drew, S.-H. Lee, K. J. Senecal, J. Kumar and L. A. Samuelson, Electrospun nanofibrous membranes for highly sensitive optical sensors, *Nano Lett.*, 2002, **2**(11), 1273–1275.
77 Y. Li, M. A. Abedalwafa, L. Tang, and L. Wang, Electrospun nanofibers for sensors, in *Electrospinning: Nanofabrication and Applications*, Elsevier, 2019, pp. 571–601.
78 J. V. Patil, S. S. Mali, A. S. Kamble, C. K. Hong, J. H. Kim and P. S. Patil, Electrospinning: A versatile technique for making of 1D growth of nanostructured nanofibers and its applications: An experimental approach, *Appl. Surf. Sci.*, 2017, **423**, 641–674.
79 S. Almuhamed, *et al.*, Electrospinning Nonwovens of Polyacrylonitrile/synthetic Na-Montmorillonite Composite Nanofibers, *J. Ind. Eng. Chem.*, 2016, **35**, 146–152.
80 P. Mehrabi, *et al.*, Fabrication of SnO_2 composite nanofiber-based gas sensor using the electrospinning method for tetrahydrocannabinol (THC) detection, *Micromachines*, 2020, **11**(2), 190.
81 G. Korotcenkov, Electrospun metal oxide nanofibers and their conductometric gas sensor application. Part 2: Gas sensors and their advantages and limitations, *Nanomaterials*, 2021, **11**(6), 1555.
82 C. H. Kim, Y. H. Jung, H. Y. Kim, D. R. Lee, N. Dharmaraj and K. E. Choi, Effect of collector temperature on the porous structure of electrospun fibers, *Macromol. Res.*, 2006, **14**, 59–65.
83 P. Supaphol and S. Chuangchote, On the electrospinning of poly (vinyl alcohol) nanofiber mats: a revisit, *J. Appl. Polym. Sci.*, 2008, **108**(2), 969–978.
84 D. Li, Y. Wang and Y. Xia, Electrospinning nanofibers as uniaxially aligned arrays and layer-by-layer stacked films, *Adv. Mater.*, 2004, **16**(4), 361–366.
85 T. Phachamud and M. Phiriyawirut, Physical properties of polyvinyl alcohol electrospun fiber mat, *Res. J. Pharm., Biol. Chem. Sci.*, 2011, **2**, 675–684.
86 A. Abd El-aziz, A. El-Maghraby and N. A. Taha, Comparison between polyvinyl alcohol (PVA) nanofiber and polyvinyl alcohol (PVA) nanofiber/hydroxyapatite (HA) for removal of Zn^{2+} ions from wastewater, *Arabian J. Chem.*, 2017, **10**(8), 1052–1060.
87 W. Ding, S. Wei, J. Zhu, X. Chen, D. Rutman and Z. Guo, Manipulated electrospun PVA nanofibers with inexpensive salts, *Macromol. Mater. Eng.*, 2010, **295**(10), 958–965.
88 Y. Zhang, X. He, J. Li, Z. Miao and F. Huang, Fabrication and ethanol-sensing properties of micro gas sensor based on electrospun SnO_2 nanofibers, *Sens. Actuators, B*, 2008, **132**(1), 67–73.
89 P. Jaroenapibal, P. Boonma, N. Saksilaporn, M. Horprathum, V. Amornkitbamrung and N. Triroj, Improved NO_2 sensing performance of electrospun WO_3 nanofibers with silver doping, *Sens. Actuators, B*, 2018, **255**, 1831–1840.
90 L. Liao, *et al.*, Size dependence of gas sensitivity of ZnO nanorods, *J. Phys. Chem. C*, 2007, **111**(5), 1900–1903.
91 J. Gao, *et al.*, One-step synthesis of mesoporous Al_2O_3–In_2O_3 nanofibres with remarkable gas-sensing performance to NO_x at room temperature, *J. Mater. Chem. A*, 2014, **2**(4), 949–956.
92 N. Sun, *et al.*, Highly sensitive and lower detection-limit NO_2 gas sensor based on Rh-doped ZnO nanofibers prepared by electrospinning, *Appl. Surf. Sci.*, 2023, **614**, 156213, DOI: 10.1016/j.apsusc.2022.156213.
93 P. Su, W. Li, J. Zhang and X. Xie, Chemiresistive gas sensor based on electrospun hollow SnO_2 nanotubes for detecting NO at the ppb level, *Vacuum*, 2022, **199**, 110961.
94 C. Yang, *et al.*, Indium element-induced oxygen vacancies and polycrystalline structure enabled SnO_2 nanofibers for highly sensitive detection of NO_x, *Sens. Actuators, B*, 2022, **362**, 131754.
95 M. Bonyani, S. M. Zebarjad, K. Janghorban, J.-Y. Kim, H. W. Kim and S. S. Kim, Au-Decorated Polyaniline-ZnO Electrospun Composite Nanofiber Gas Sensors with Enhanced Response to NO_2 Gas, *Chemosensors*, 2022, **10**(10), 388.
96 Z. Ma, K. Yang, C. Xiao and L. Jia, Electrospun Bi-doped SnO_2 porous nanosheets for highly sensitive nitric oxide detection, *J. Hazard. Mater.*, 2021, **416**, 126118.
97 A. Katoch, Z. U. Abideen, J.-H. Kim and S. S. Kim, Influence of hollowness variation on the gas-sensing properties of ZnO hollow nanofibers, *Sens. Actuators, B*, 2016, **232**, 698–704.
98 Z. U. Abideen, A. Katoch, J.-H. Kim, Y. J. Kwon, H. W. Kim and S. S. Kim, Excellent gas detection of ZnO nanofibers by loading with reduced graphene oxide nanosheets, *Sens. Actuators, B*, 2015, **221**, 1499–1507.
99 E. Zampetti, *et al.*, A high sensitive NO_2 gas sensor based on PEDOT–PSS/TiO_2 nanofibres, *Sens. Actuators, B*, 2013, **176**, 390–398.
100 O.-K. Kim, H. Kim and D. Kim, Electrospun non-directional zinc oxide nanofibers as nitrogen monoxide gas sensor, *Korean J. Mater. Res.*, 2012, **22**(11), 609–614.
101 I. D. Kim and A. Rothschild, Nanostructured metal oxide gas sensors prepared by electrospinning, *Polym. Adv. Technol.*, 2011, **22**(3), 318–325.
102 Q. Gao, J. Luo, X. Wang, C. Gao and M. Ge, Novel hollow α-Fe_2O_3 nanofibers *via* electrospinning for dye adsorption, *Nanoscale Res. Lett.*, 2015, **10**, 1–8.
103 C. Yan, *et al.*, Synthesis of porous NiO-In_2O_3 composite nanofibers by electrospinning and their highly enhanced gas sensing properties, *J. Alloys Compd.*, 2017, **699**, 567–574.
104 J. Zhang, H. Lu, C. Liu, C. Chen and X. Xin, Porous NiO–WO_3 heterojunction nanofibers fabricated by electrospinning with enhanced gas sensing properties, *RSC Adv.*, 2017, **7**(64), 40499–40509.

105 S.-H. Choi, *et al.*, Hollow ZnO nanofibers fabricated using electrospun polymer templates and their electronic transport properties, *ACS Nano*, 2009, **3**(9), 2623–2631.
106 Y. Bakha and H. Khales, Zinc Oxide Thin Film Prepared by Micro-Dropping Chemical Method on QCM for Gas Sensing, *Acta Phys. Pol., A*, 2019, **136**(3), 490–494.
107 M. Berouaken, *et al.*, Quartz Crystal Microbalance Coated with Vanadium Oxide Thin Film for CO_2 Gas Sensor at Room Temperature, *Arabian J. Sci. Eng.*, 2018, **43**, 5957–5963.
108 N. Rahman, *et al.*, Insight into metallic oxide semiconductor (SnO_2, ZnO, CuO, α-Fe_2O_3, WO_3)-carbon nitride (g-C_3N_4) heterojunction for gas sensing application, *Sens. Actuators, A*, 2021, **332**, 113128.
109 S. Bai, *et al.*, On the construction of hollow nanofibers of ZnO-SnO_2 heterojunctions to enhance the NO_2 sensing properties, *Sens. Actuators, B*, 2018, **266**, 692–702.
110 J. Su, X.-X. Zou, Y.-C. Zou, G.-D. Li, P.-P. Wang and J.-S. Chen, Porous titania with heavily self-doped Ti^{3+} for specific sensing of CO at room temperature, *Inorg. Chem.*, 2013, **52**(10), 5924–5930.
111 D. V. Ponnuvelu, S. Abdulla and B. Pullithadathil, Novel Electro-Spun Nanograined ZnO/Au Heterojunction Nanofibers and Their Ultrasensitive NO_2 Gas Sensing Properties, *ChemistrySelect*, 2018, **3**(25), 7156–7163.
112 K. Nguyen, *et al.*, Low-temperature prototype hydrogen sensors using Pd-decorated SnO_2 nanowires for exhaled breath applications, *Sens. Actuators, B*, 2017, **253**, 156–163.
113 B.-H. Jang, O. Landau, S.-J. Choi, J. Shin, A. Rothschild and I.-D. Kim, Selectivity enhancement of SnO_2 nanofiber gas sensors by functionalization with Pt nanocatalysts and manipulation of the operation temperature, *Sens. Actuators, B*, 2013, **188**, 156–168.
114 C. Zhao and H. Wu, A first-principles study on the interaction of biogas with noble metal (Rh, Pt, Pd) decorated nitrogen doped graphene as a gas sensor: A DFT study, *Appl. Surf. Sci.*, 2018, **435**, 1199–1212.
115 P. Gouma, A. Prasad and S. Stanacevic, A selective nanosensor device for exhaled breath analysis, *J. Breath Res.*, 2011, **5**(3), 037110.
116 J. Zhang, *et al.*, Porosity and oxygen vacancy engineering of mesoporous WO3 nanofibers for fast and sensitive low-temperature NO_2 sensing, *J. Alloys Compd.*, 2021, **853**, 157339.
117 N. M. Hung, *et al.*, Carbon nanotube-metal oxide nanocomposite gas sensing mechanism assessed *via* NO_2 adsorption on n-WO3/p-MWCNT nanocomposites, *Ceram. Int.*, 2020, **46**(18), 29233–29243.
118 R. Yoo, *et al.*, Selective detection of nitrogen-containing compound gases, *Sensors*, 2019, **19**(16), 3565.
119 J. Moon, J.-A. Park, S.-J. Lee, T. Zyung and I.-D. Kim, Pd-doped TiO_2 nanofiber networks for gas sensor applications, *Sens. Actuators, B*, 2010, **149**(1), 301–305.
120 C. Kuchi, B. Naresh and P. S. Reddy, In situ TiO_2-rGO nanocomposite for low concentration NO gas sensor, *ECS J. Solid State Sci. Technol.*, 2021, **10**(3), 037008.
121 K. Yoo, K. Kang, Y. Chen, K. Han and J. Kim, The TiO_2 nanoparticle effect on the performance of a conducting polymer Schottky diode, *Nanotechnology*, 2008, **19**(50), 505202.
122 D. Levaggi, E. L. Kothny, T. Belsky, E. De Vera and P. K. Mueller, Quantitative analysis of nitric oxide in presence of nitrogen dioxide at atmospheric concentrations, *Environ. Sci. Technol.*, 1974, **8**(4), 348–350, DOI: 10.1021/es60089a003.
123 R. A. Dweik, *et al.*, An official ATS clinical practice guideline: interpretation of exhaled nitric oxide levels (FENO) for clinical applications, *Am. J. Respir. Crit. Care Med.*, 2011, **184**(5), 602–615.
124 P. Luo, M. Xie, J. Luo, H. Kan and Q. Wei, Nitric oxide sensors using nanospiral ZnO thin film deposited by GLAD for application to exhaled human breath, *RSC Adv.*, 2020, **10**(25), 14877–14884.